

STUDY OF SI(AL)CN FUNCTIONALIZED CARBON NANOTUBE COMPOSITE AS A
HIGH TEMPERATURE THERMAL ABSORBER COATING MATERIAL.

by

DEEPU ASOK

B.Tech., University of Kerala, 2010

A REPORT

Submitted in partial fulfillment of the requirements for the degree

MASTER OF SCIENCE

Department of Mechanical & Nuclear Engineering
College of Engineering

KANSAS STATE UNIVERSITY
Manhattan, Kansas

2013

Approved by:

Major Professor
Dr.Gurpreet Singh

Abstract

Carbon nanotubes (CNT) and polymer-derived ceramics (PDC) have gained considerable research attention due to their unique structure and physical properties. Carbon nanotubes are known for their exceptional mechanical (Young's modulus= 1 TPa) and thermal properties (thermal conductivity = 4000 W/m.K). However, CNTs tend to lose their unique sp^2 carbon structure and cylindrical geometry at temperatures close 400°C in air. PDC, which are obtained by the controlled degradation of certain organosilicon polymers however exhibit high temperature stability (upto approx. 1400 °C). To this end, a hybrid composite material consisting of PDC functionalized CNT is of interest as it can combine the unique physical properties of the two materials for applications requiring operation under harsh conditions.

Here, we report synthesis and chemical characterization of an Al-modified polysilazane polymer, which was later utilized to functionalize the outer surfaces of four commercially available CNTs. This polymer-CNT composite upon heating in nitrogen environment resulted in Si(Al)CN-CNT ceramic composite. The composite was characterized using a variety of spectroscopic methods such Raman, FTIR and electron microscopy. The thermal stability of the ceramic composite was studied by use of Thermogravimetric analysis (TGA) that showed an improvement in the thermal stability compared to bare nanotubes. Further, we also demonstrate that a stable dispersion of the composite in organic solvents such as toluene can be spray coated on a variety of substrates such as copper disks and foils. Such coatings have application in high energy laser power meters.

This research opens new avenues for future applications of this novel material as coatings on surfaces that require both good thermal properties and protection against degradation in high

temperature environments. We also suggest the future use of this material as an electrode material in high electrochemical capacity rechargeable batteries.

Table of Contents

List of Figures	vi
List of Tables	ix
Acknowledgements.....	x
Dedication.....	xi
Introduction.....	1
Chapter 1 -Polymer Derived Ceramics.....	3
1.1 Polymer Derived Ceramics	3
1.2 Polymer Synthesis.....	4
1.3 Polymer to Ceramic Conversion	7
1.3.1 Cross linking of the preceramic polymer	8
1.3.2 Ceramization process	9
1.4 Polymer Derived Ceramic Structure	10
1.5 Tunable Thermal Properties.....	11
1.6 Carbon Nanotubes.....	13
1.6.1 Properties of carbon nanotubes	15
1.6.2 Engineering applications.....	16
1.7 Polymer Derived Ceramic Structure	16
1.8 Application: Laser Thermal Detector Coatings	20
1.9 References.....	24
Chapter 2 - Study of Si(Al)CN Functionalized Carbon Nanotube Composite as a High Temperature Thermal Absorber Coating Material	29
2.1 Introduction.....	29
2.2 Preparation of the Pre-Ceramic Polymer	29
2.3 Conventional Pyrolysis	31
2.4 Microwave Pyrolysis	33
2.5 Characterization	34
2.5.1 Electron microscopy	35
2.5.2 Thermogravimetric analysis.....	36
2.5.3 Raman spectroscopy	39

2.5.4	X-ray photoelectron spectroscopy	40
2.6	Preparation of Coatings.....	43
2.7	References.....	46
Chapter 3 - Conclusion and Future Work		47

List of Figures

Figure 1-1: A schematic showing the general structure of an organosilicon polymer [5].....	4
Figure 1-2: A timeline showing the important inventions and findings in the history of PDC.	7
Figure 1-3: A schematic showing (a) The free flowing individual polymer chains before the cross linking process and (b) The cross-linked polymer chains formed upon heating.	8
Figure 1-4: The major reactions involved in the polymer to ceramic conversion process namely (a) Transamination (b) Dehydrocoupling (c) Vinyl polymerization (d) Hydrosilylation.	9
Figure 1-5: Nanodomain structure of Si(Al)CN Ceramics obtained from polysilazanes.....	11
Figure 1-6: High temperature thermal stability comparison of Si_3N_4 with PDC-SiCN and SiBCN [12].....	12
Figure 1-7: (a) A schematic of a single wall carbon nanotube is shown on the left and multi-walled carbon nanotube is shown on the right. The interplanar distance is shown as 0.36 nm [17]. (b) A representation of the chirality of carbon nanotubes. The chirality of the nanotubes depends on the unit vectors m and n [17].	14
Figure 1-8: TEM (Transmission electron microscope) image of carbon nanotubes (Manufacturer: Nanocyl) taken at Kansas State University with magnifications of (a) 245000X and (b) 130000X. The tubular structures seen are the individual carbon nanotubes.....	14
Figure 1-9: A schematic of the various methods of production of carbon nanotubes.	15
Figure 1-10: SEM images of (a) Single wall nanotube bundle (b) Entangled multiwall carbon nanotube agglomerates [26].....	17
Figure 1-11: A schematic showing the various non-covalent functionalization methods (a): polymer wrapping (b) Surfactant adsorption (c) Endohedral method [26].....	18

Figure 1-12: (a-b) SEM image of fracture surface of SiCN/CNT composite with 10 and 5 vol % CNT respectively [28], [29]. (c-d) SEM image of SiCN/MWCNT composite nanowires [30]... 19

Figure 1-13: Cutaway diagram of the flowing-water thermal detector, illustrating the absorbing 21

Figure 1-14: (a) A cone cavity coated with carbon nanotubes as the coating material [38]. (b) A schematic showing the conduction type liquid flowing type calorimeter with various parts labeled [39]. 21

Figure 2-1: Proposed reaction mechanism for molecular level interfacing of Aluminium with poly(ureamethylvinyl)silazane liquid polymer. 30

Figure 2-2: Schematic showing the preparation of the CNT-Preceramic polymer mixture 31

Figure 2-3: Graph showing the heating rates during the cross-linking and pyrolysis of the preceramic polymer. 32

Figure 2-4: Schematic showing the conventional pyrolysis of the CNT-Polymer mix in the tube furnace with flowing nitrogen..... 32

Figure 2-5: A photograph showing the experimental setup for the microwave pyrolysis of the preceramic polymer. The black material at the bottom of the test tube is the CNT-Polymer mix. The yellow fumes seen indicate the release of ammonia..... 34

Figure 2-6: TEM images (a) bare nanotubes (b) Polymer coated nanotubes (c) Nanotube-ceramic prepared by the conventional method (d) CNT-ceramic prepared by microwave pyrolysis..... 36

Figure 2-7: (a) TGA plots showing the weight loss (%) and oxidation temperature (°C) for MWCNT, Si(Al)CN-MWCNT prepared by conventional heating, Si(Al)CN-MWCNT prepared by microwave heating and MWCNTs performed in flowing air..... 38

Figure 2-8: TGA plots showing the weight loss (%) and oxidation temperature (°C) for the two varieties of Si(Al)CN-MWCNT composites prepared by using two commercially available MWCNT (Manufacturer1: Nanocyl and Manufacturer2: Arkema), synthesized through both conventional and microwave heating..... 38

Figure 2-9: Raman spectra of the as prepared Si(Al)CN/CNT composite. The Raman plot of Si(Al)CN-MWCNT ceramic composite powder indicates the presence of D (~1350 cm⁻¹) and G (~1600 cm⁻¹) bands (peaks) that are characteristic of carbon nanotubes (CNT). 40

Figure 2-10: High resolution Al_{2p} XPS spectrum. The peak at 74.4 eV is indicative of the presence of Al-N bonds in the final ceramic. 42

Figure 2-11: High resolution C_{1s} XPS spectrum indicating the presence of sp² bonded graphitic carbon at around 284.5 eV. 42

Figure 2-12: High resolution Si_{2p} XPS spectrum of the composite material shows a characteristic peak at 101.8 eV indicating the presence of Si₃N₄..... 43

Figure 2-13: Photograph showing the dispersions of Si(Al)CN-MWCNT composite powder in toluene prepared by using four different commercially available makes of MWCNTs (a) Si(Al)CN-C Nano #1 b) Si(Al)CN-Nanocyl c) Si(Al)CN-C Nano #2 d) Si(Al)CN-Arkema

Figure 2-14: A schematic showing the spray coating of the copper disks with the as prepared CNT-Ceramic composite. (Inset is the SEM image of the coating showing the uniform distribution of the particles on the surface of the coating)..... 44

Figure 2-15: A photograph showing the four Si(Al)CN-MWCNT coatings prepared by using four different commercially available makes of MWCNTs. This would help in comparing the effect of different varieties of CNT on the thermal performance of the coating. 44

List of Tables

Table 1-1: Various properties of PDC-CNT composites studied previously..... 20

Table 1-2: Desired properties for the thermal absorbent coating materials for laser power meters.

..... 22

Acknowledgements

I would like to express my deep gratitude to my Advisor, Dr. Gurpreet Singh for giving me the opportunity to work on this research project. I am extremely grateful to him for continuously supporting me and providing me with valuable comments and suggestions along the course of my master's degree. I would also like to thank my advisory committee members Dr. Don Fenton and Dr. Byron Jones for willing to be on my committee and for their patient guidance and encouragement.

I would like to thank the following people for providing access to various characterization equipments: Dr. Leila Maurmann, Dr. Hongwang Wang.

I am extremely thankful to my colleague Lamuel David for his assistance with various characterization techniques and generous support during the course of my research.

I am thankful to my parents, sister and brother-in-law for their unconditional love and prayers that has strengthened me during the tough times. Finally I wish to thank my friend Anusha for being there to support and encourage me throughout my study at Kansas State University.

This research is based on work supported by the National Science Foundation (Chemical, Bioengineering, Environmental, and Transport Systems Division), under grant no. 1335862 to G. Singh.

Dedication

To my dear parents for their love and support.

Introduction

Copper cone-type calorimeters/thermal detectors are used as measurement standards for high power lasers and for lasers used in the manufacturing industry. The interior of the copper cavity is coated with a high optical/thermal absorbent coating to convert the incident radiation energy to thermal energy. A suitable coating material would be one which possesses the desired properties such as 1) High thermal conductivity for the conduction of the absorbed heat to the substrate 2) Maximum absorption in the visible to infrared spectrum for accurate response and to prevent coating damage due to attenuation of the laser radiation and 3) High visual damage threshold (for high power lasers). Keeping these requirements in mind, several coating materials have been studied previously such as carbon black and black metallic coatings (eg: gold black) due to their ability to absorb a wide range of wavelengths (up to $40\mu\text{m}$) [1]. In spite of the good absorption properties, these materials are not suited for high power laser radiometry because of their poor laser damage threshold (or oxidation resistance) and non-uniform spectral response with reflectance. Recently multiwall carbon nanotubes (MWCNT) based coatings have been reported as promising, due to their uniform spectral absorbance from visible to IR wavelengths, high thermal conductivity, and a high laser damage threshold of around $15 \text{ kW}\cdot\text{cm}^{-2}$ at $1.06 \mu\text{m}$ exposure [2]. However the damage threshold values of MWCNTs are greatly reduced ($1.4 \text{ kW}\cdot\text{cm}^{-2}$) at $10.6\mu\text{m}$ exposure.

A solution for this problem would be to improve the laser damage resistance of MWCNTs (at $10.6\mu\text{m}$ exposure) by functionalizing their surfaces with a high oxidation resistant material such as the polymer derived Si(Al)CN ceramic. Polymer derived Si(Al)CN ceramic which is produced by the controlled thermal decomposition (pyrolysis) of liquid polymer (such as Aluminium

doped polysilazane) is stable upto 1400°C [3]. The Al-modified Polymeric precursor can be interfaced with CNTs, to yield a core/shell type composite structure upon heating. In addition to oxidation resistance, the core/shell composite is also likely to exhibit high thermal conductivity and optical absorbance contributed by both the nanotube core and the sp^2 bonded free carbon present in the Si(Al)CN ceramic shell. Also the single step synthesis of Si(Al)CN-CNT composite will allow the preparation of the material in large quantities (in grams). This would allow the deposition of the material on large areas using simple spray coating techniques, such as the large interior surface of the copper cavity in laser power meters. Consequently, in this report we were motivated to prepare spray coatings of Si(Al)CN-MWCNT composite for potential application in high power radiometry, especially at 10.6 μm exposure.

Chapter 1 -Polymer Derived Ceramics

1.1 Polymer Derived Ceramics

Polymer derived ceramics (PDCs) are advanced ceramic materials which are synthesized by the pyrolysis of organometallic polymers. PDCs were first made in the 1960's as non-oxide ceramics starting from molecular precursors. The first successful transformations of polyorganosilicon compounds (polysilazanes, polysiloxanes, and polycarbosilanes) to ceramic materials was done around 10 years after, to manufacture $\text{Si}_3\text{N}_4/\text{SiC}$ ceramic fibers for high temperature applications [4]. Later Fritz & Raabe and Yajima et al. synthesized SiC ceramics from polycarbosilanes almost at the same time, which was a significant leap in the science of PDCs. Polymer Derived Ceramics are basically classified based on the number of constituent elements of the resulting ceramic material. Binary Systems Si_3N_4 , SiC, BN and AlN, Ternary systems SiCN, SiCO and BCN, Quaternary systems SiCNO, SiBCN, SiBCO, Si(Al)CN, and SiAlCO have been widely investigated. A unique feature of polymer derived ceramics which makes them more favorable than the non-polymer route is its ability to be synthesized at a much lower temperature range of 1100°C – 1300°C . In comparison to the traditional ceramic manufacturing procedures, that involve sintering processes which require a temperature range of 1700°C – 2000°C and high pressurization of the starting powders, the polymer precursor route proves to be more economical. The PDCs also offer much more flexibility in the shapes and forms in which ceramics can be produced compared to the traditional methods. The polymers can be shaped using polymer infiltration pyrolysis (PIP), injection molding, coating from solvent, extrusion, or resin transfer molding (RTM) and subsequently heated to obtain the final ceramic product. This unique feature allows us to make ceramic fibers, layers and composite materials. The most striking feature about polymer derived ceramics (especially in ternary and above) is its ability to

resist crystallization during the heating process, resulting in amorphous structures with three dimensional nanodomain networks consisting of Si-C, Si-N and Si-O bonds. The enthalpies of formations for the amorphous ceramics are much higher than their crystalline counterparts. This unique feature makes the structure thermodynamically more stable than its crystalline counterparts produced through the traditional methods and hence finds applications in high temperature scenarios like glow plugs, high speed brakes, laser detectors etc.

1.2 Polymer Synthesis

Silicon based pre-ceramic polymers consist of repetitive chains of silicon based monomers with general structure as shown below.

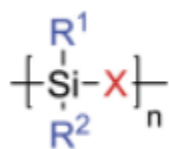
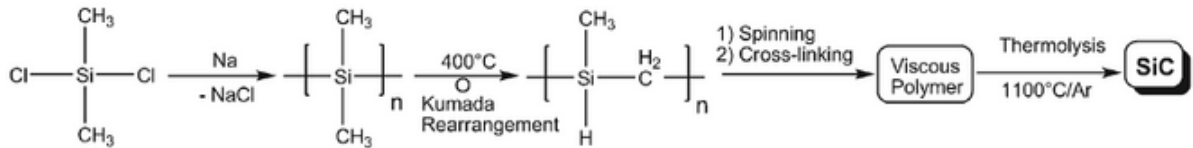


Figure 1-1: A schematic showing the general structure of an organosilicon polymer [5].

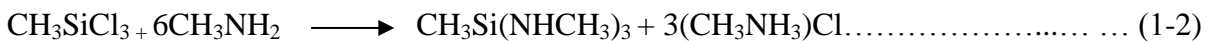
As shown in Fig 1-1, R^1 and R^2 will be organic functional groups and $-X-$ will be mostly $-O-$, $-C-$ or $-N-$. The polymer pre-cursor can be varied to obtain different properties for the final ceramic. For example the variation of the group (X) in the general structure can give result to various classes of precursors such as polyorganosilanes ($X=Si$), polyorganocarbosilanes ($X=CH_2$), polyorganosilazanes ($X=NH$), polyorganosilylcarbodiimides ($X=[N=C=N]$). The selection of the organic groups on the branches can affect various properties of the precursor polymer such as thermal stability, optical, electronic and rheological properties. The carbon content in the preceramic polymer can also be controlled by the functional groups attached to Si. The synthesis of a binary polymer precursor was first introduced through the early works of Yajima et al. in the

1970s when they obtained polycarbosilanes starting from dimethyldichlorosilanes. They demonstrated the production of Si-C based ceramic fibers through the thermolysis of polycarbosilanes as shown in equation 1-1 [4].

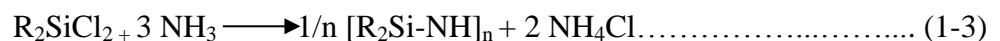


..... (1-1)

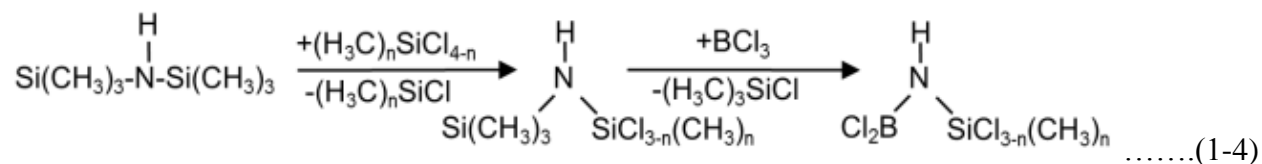
In 1974 Verbeek of Bayer AG developed a precursor for Si₃N₄/SiC based on the reaction product of methyl trichlorosilane and methylamine as shown in equation 1-2 [6].



The synthesis of quaternary PDC systems were demonstrated by Takamizawa et al. in 1984 using a single polymeric precursor [7]. The method involved the reaction of polymethylsilane with B-trimethyl-N-triphenyl borazine. The thermal treatment of the above mixture resulted in the decomposition and polycondensation reactions yielding Si-B-C-N Ceramic. Another popular method for the synthesis of polyborosilazane or polycarbosilazane was by the hydroboration of single source precursors with chlorine substituents, and nitrogen containing (methylamine) compounds as crosslinking agents followed by the condensation and deamination as shown in equation 1-3, [4].



the problem with this method was that, in the ammonolysis reaction, large quantities of ammonium chloride were produced, which had to be removed from the resulting reaction mixture. Since polysilazanes decompose in the presence of water or moisture, this removal of ammonium chloride was usually carried out in a dry organic solvent and the ammonium chloride is removed through filtration of the reaction mass. Various other methods were later developed to overcome this cumbersome and cost-intensive filtration step and to avoid the formation of any solid materials like ammonium chloride in the final step. Another method was developed by Abel et al for Commodore/KiON for the synthesis of polysilazanes [8]. This method comprises introducing a starting compound containing at least one Si-H bond, such as a halosilane into a stoichiometric excess of anhydrous liquid ammonia wherein an ammonium halide is generated acting as an acid catalyst to provide an ionic and/or acidic environment for preparing the novel ammonolysis compounds. The resulting ammonium halide dissolves in the liquid ammonia and is retained in a separated liquid-phase layer and distinct from the ammonolysis products. When hexamethyldisilazane or HDMS $[(CH_3)_3Si]_2NH$ can be used as a nitrogen source instead of ammonia, transamination (Amine (NH_2) group on one molecules is replaced by a keto $(=O)$ group on the other molecule) takes place. In this method the chlorine liberated was attached to the trimethylsilyl groups of HDMS so that no chlorine containing solid salts are formed. The process is shown in equation 1-4. A history of the major findings are shown in Fig 1-2




- 
- 1940s** - Polysilazanes were synthesized using chlorosilanes [5].
- 1960s** - P. Popper & P. Chantrell made Si-based ceramics from organometallic polymers [4].
- 1970s** - Verbeek synthesized SiCN fibers with enhanced performance [6].
- 1989** - Blum & Co. synthesized PDCs by pyrolysis of Polysilazanes [9].
- 1990** - Seyferth et al. synthesized quaternary SiBCN using cyclic oligomers [10].
- 1993** - Crack free SiCN ceramics were synthesized by Riedel & Co [11].
- 1996** - Riedel et al. showed high thermal stability for SiBCN upto 2000°C [12].
- 2001** - Hermann et al. co-related the structural & electronic properties of SiBCN ceramics [11].
- 2003** - Liew et al. fabricated MEMS actuator using SiCN [13].
- 2004** - Linan et al. synthesized SiCN-CNT composite [14].

Figure 1-2: A timeline showing the important inventions and findings in the history of PDC.

1.3 Polymer to Ceramic Conversion

The polymer to ceramic conversion process basically involves two major steps

1. Cross-linking of the polymers at moderate temperatures (around ~400°C) to form an infusible material.
2. Ceramization (pyrolysis) at temperatures ranging from 1000°C to 1300°C of the cross linked materials which converts the organic polymer to an amorphous inorganic ceramic material

1.3.1 Cross linking of the preceramic polymer

The cross linking process is a very important step in the synthesis of polymer derived ceramics. It involves the conversion of the polymeric precursor into organic/inorganic materials at low temperatures (100°C to 400°C). The liquid polymer (which consists of free flowing chains) can be turned into solid/gel by cross-linking the chains together. The crosslinking process also ensures the retention of low molecular weight components of the polymeric precursor and thus increases the ceramic yield. Hence the crosslinking process enables the conversion of a liquid starting material to a solid infusible material which retains its shape during the ceramization process without melting. This provides the user with a flexibility to shape the final ceramic according to the required application.

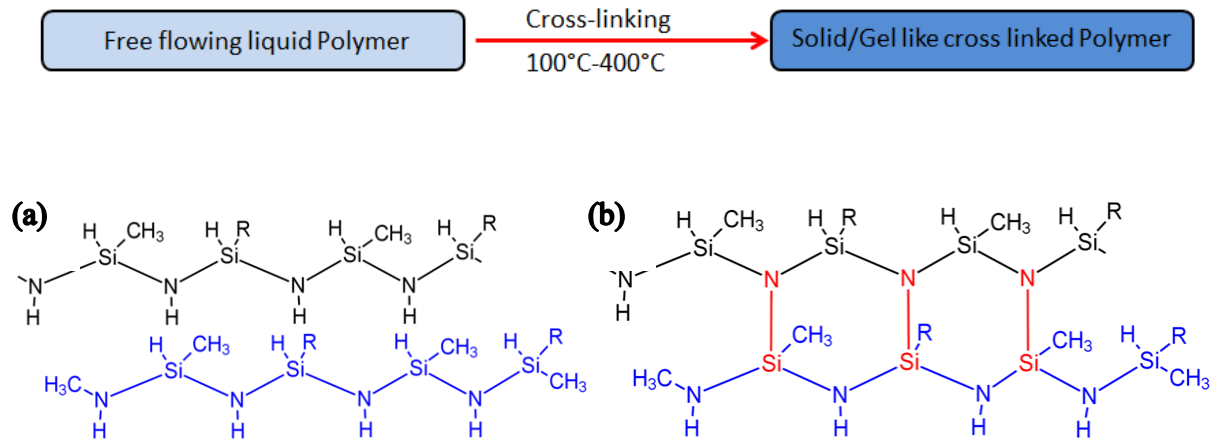


Figure 1-3: A schematic showing (a) The free flowing individual polymer chains before the cross linking process and (b) The cross-linked polymer chains formed upon heating.

The cross linking of polysilazanes can be achieved thermally, or by using chemical reagents such as catalysts or peroxides. There are four major reactions that enable the cross-linking of the polymers. They are shown in Fig 1-4.

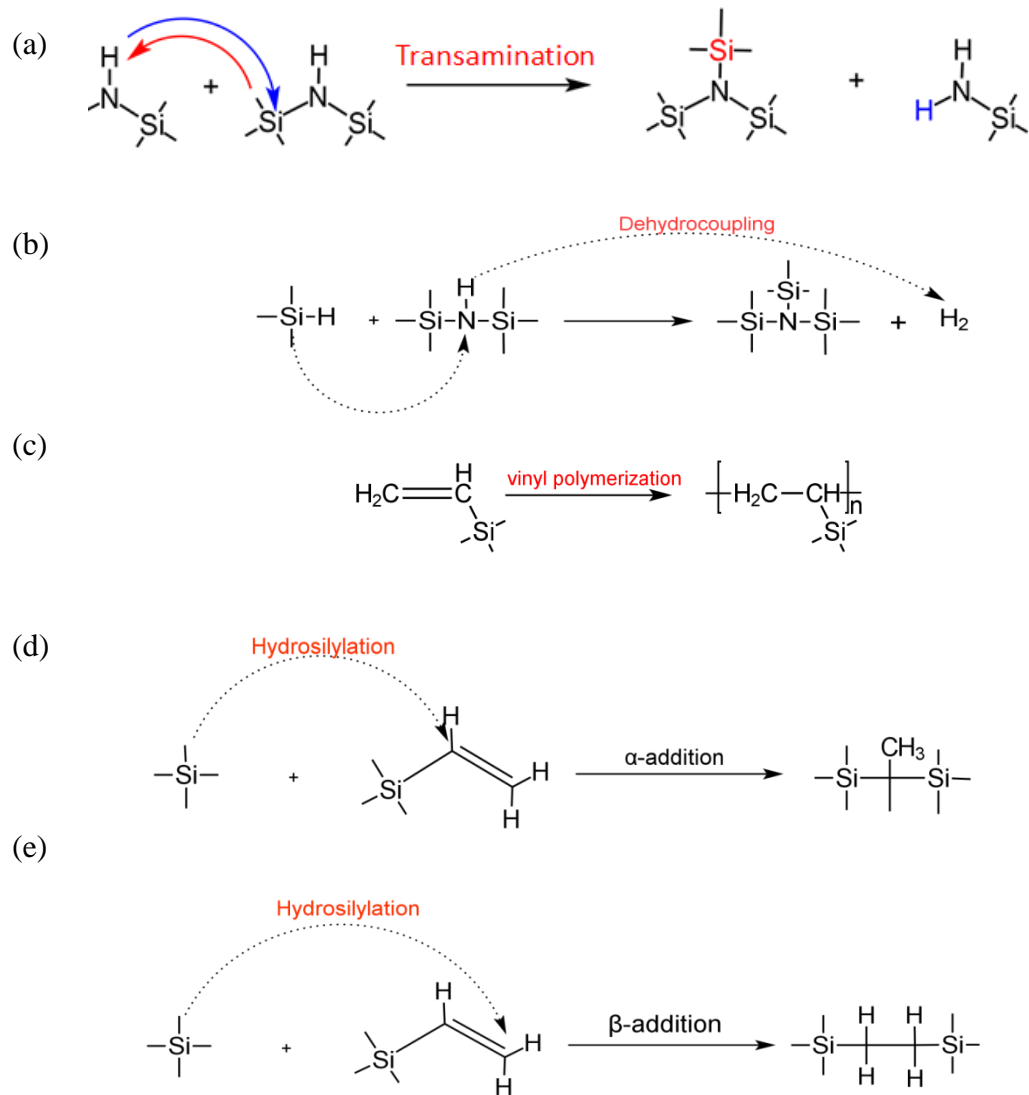


Figure 1-4: The major reactions involved in the polymer to ceramic conversion process namely (a) Transamination (b) Dehydrocoupling (c) Vinyl polymerization (d) Hydrosilylation.

1.3.2 Ceramization process

The polymer to ceramic conversion of the preceramic polymer involves the pyrolysis which results in the volatilization of organic groups in the structure at high temperatures (600°C to 1000°C). This results in the complete transformation of the organic polymer to an amorphous inorganic ceramic. The material shows weight loss before and after the pyrolysis process. This

weight loss is mainly attributed to the release of gases which are formed due to the various reactions at different temperature ranges. The weight loss at lower temperatures (<500°C) is due to the evaporation of the oligomers due to hydrosilylation and the release of ammonia gas due to transamination. At higher temperature the evolution of hydrocarbons (e.g. CH₄, C₂H₆ etc.) and hydrogen results in further weight loss. The temperature at which the various weight losses occur is governed by the chemistry of the polymeric precursor and the heating rates. The carbon present in the precursor is either released at about 600°C - 800°C or is retained in the form of turbostratic carbon and other carbon bound to parent silicon atoms. The presence and the distribution of carbon in the final polymer derived ceramic material can influence the properties such as thermal stability, electrical conductivity etc. The choice of the preceramic polymer is one of the key aspects in the synthesis of polymer derived ceramics since the molecular structure of the polymeric precursor will not only affect the composition of the final ceramic but also the micro/nano phase distribution in the final ceramic matrix. Therefore the macroscopic physical and chemical properties of the polymer derived ceramic can be altered by designing the suitable polymeric precursor.

1.4 Polymer Derived Ceramic Structure

Polymer derived ceramics are amorphous covalent ceramics which result from the controlled thermal decomposition of organosilicon polymers such as polysilazanes (SiCN), polysiloxanes, polycarbosilanes, polyborosilanes etc. PDCs have been known to possess several functional properties such as high temperature stability, electrical conductivity, creep resistance and mechanical strength. The ability to vary the quantity and quality of the functional properties by varying the synthesis conditions makes PDCs a very promising material for special applications. Much of these properties are based upon the microstructure of the final material which mostly

consists of single/multiphase amorphous networks with long chains of sp^2 bonded carbon atoms (graphene) as shown in Fig 1-5.

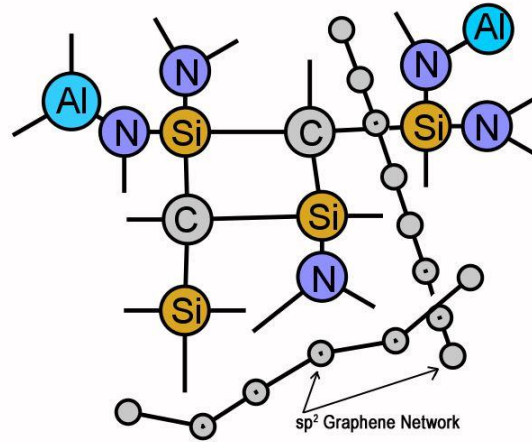


Figure 1-5: Nanodomain structure of Si(Al)CN Ceramics obtained from polysilazanes.

The single phase amorphous network contains free carbon which is seen as long chains of sp^2 bonded Graphene networks. The properties of polymer derived ceramics are mainly dependent on the temperature dependent microstructure which consists of mixed silicon bonded tetrahedras and free sp^2 carbon in the form of long chains. The microstructure of PDCs can be analyzed by use of solid state nuclear magnetic resonance spectroscopy.

1.5 Tunable Thermal Properties

The chemical composition of the preceramic polymer and the processing conditions can impact the final properties of the resulting ceramic. This gives PDCs the ability to tune the properties of the ceramic to the required application. Polymer derived ceramics such as SiCN and SiOC are thermodynamically more stable than their crystalline counterparts such as SiO_2 , SiC and Si_3N_4 as shown in Fig 1-6, which is mainly due to the presence of Si mixed bond tetrahedras and the

excess free carbon which limits atomic mobility in the ceramic resisting crystallization up to very high temperatures.

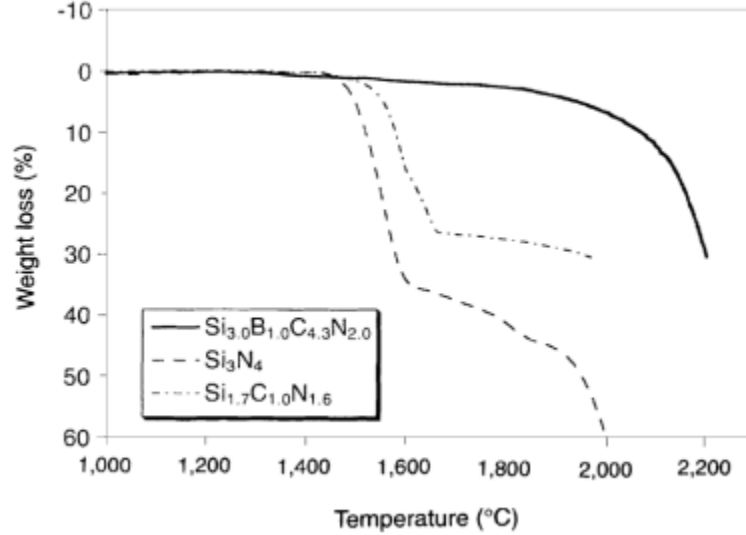


Figure 1-6: High temperature thermal stability comparison of Si₃N₄ with PDC-SiCN and SiBCN [12].

Generally the carbon rich PDCs show much higher resistance to crystallization than carbon deficient PDCs. In the case of SiCN, it is believed that the graphene like carbon wraps around Si₃N₄ domains and thereby limits the outward diffusion of nitrogen atoms. The elemental doping with elements such as B, Al, Zr and Hf has further shown to improve the resistance to crystallization and decomposition of SiCN at high temperatures. In the case of Si-B-C-N ceramics, boron is known to form a turbostratic B-C-N phase with carbon resulting in a diffusion barrier, further improving their thermal stability [9]. Addition of aluminium has known to form bonds with nitrogen and increases the nitrogen content in the final ceramic[15]. Hence thermodynamic stability in polymer derived ceramics can be improved

by elemental doping (resulting in ternary to quaternary systems) or by varying the processing conditions.

1.6 Carbon Nanotubes

Carbon nanotubes (CNTs) are considered as a new form of pure carbon which can be visualized as rolled hexagonal carbon networks that are capped by pentagonal carbon rings. There are two types of carbon nanotubes: single walled (SWNTs) and multi-walled (MWNTs). The existence of carbon nanotubes were first reported by Sumio Iijima in 1991 as helical microtubules growing on the negative electrode in an arc discharge process involving a hydrocarbon gas. [16]. The walls of CNTs are composed of sp^2 hybridized carbon-carbon bonds which are much stronger than the sp^3 hybridized bonds which are seen in diamond. The structure of CNT can be visualized as a chicken wire made up of carbon atoms which are rolled up to form a cylindrical structure as shown in Fig 1-7 (a). The TEM images are shown in Fig 1-8. The simple one atom thick planar sheet of carbon atoms are called graphene, the structure formed upon rolling up graphene is called single wall carbon nanotubes (SWCNT) and when concentric tubes of nanotubes exist coaxially they are called multiwalled carbon nanotubes (MWCNT). There is more than one way to roll up the graphene sheets, depending upon the orientation in which it is rolled, thus resulting in more than one kind of nanotube. The way the graphene sheets are rolled can be represented by a pair of indices (n,m) as shown in Fig 1-7 (b). The integers n and m denote the number of unit vectors along two directions in the honeycomb crystal lattice of graphene. If $m = 0$, the nanotubes are called zigzag nanotubes, and if $n = m$, the nanotubes are called armchair nanotubes. Otherwise, they are called chiral. The chirality of the nanotubes can also play an important role in their physical and chemical properties.

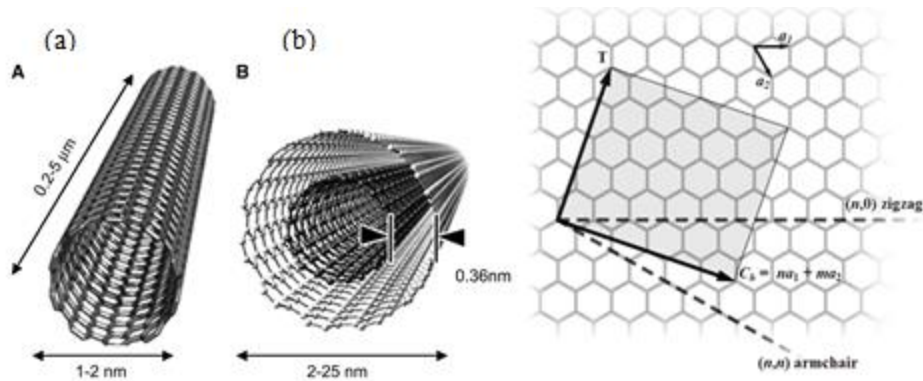


Figure 1-7: (a) A schematic of a single wall carbon nanotube is shown on the left and multi-walled carbon nanotube is shown on the right. The interplanar distance is shown as 0.36 nm [17]. (b) A representation of the chirality of carbon nanotubes. The chirality of the nanotubes depends on the unit vectors m and n [17].

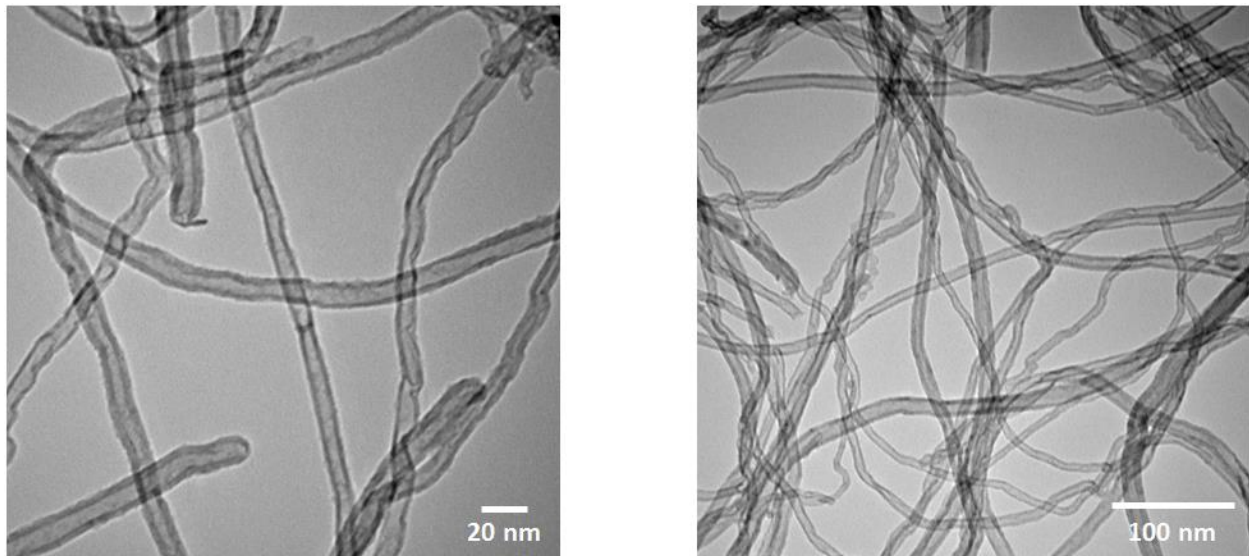


Figure 1-8: TEM (Transmission electron microscope) image of carbon nanotubes (Manufacturer: Nanocyl) taken at Kansas State University with magnifications of (a) 245000X and (b) 130000X. The tubular structures seen are the individual carbon nanotubes.

The major methods of synthesis of carbon nanotubes are the bottom up approaches as shown in Fig 1-9.

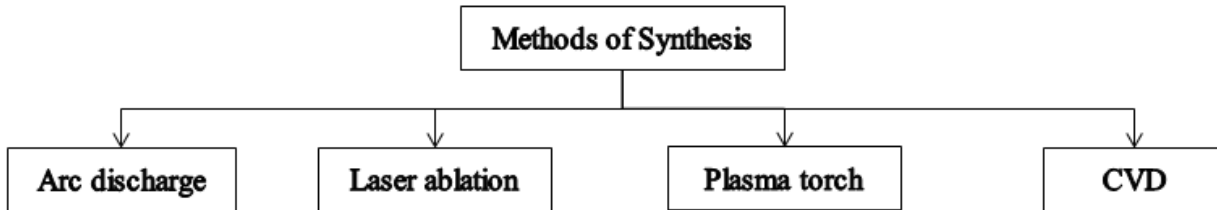


Figure 1-9: A schematic of the various methods of production of carbon nanotubes.

1.6.1 Properties of carbon nanotubes

CNTs are basically classified depending on their diameter and chirality which influences their physical properties. SWCNTs can be either semiconductor or quasi-metallic. Band gaps varying from ~ 0.5 eV to 10 meV have been reported for tubes with identical (~ 1.5 nm) diameters depending on their chirality. MWCNTs on the other hand usually exhibit semiconducting behavior [18]. The mechanical properties of CNTs in the clustered form or with a few structural defects are mainly investigated by the use of high resolution transmission electron microscopy (HRTEM), scanning transmission electron microscopy (STEM) or by atomic force microscopy (AFM). As known from previous results the graphite in-plane modulus (1.06 TPa), C-C bond properties (130 GPa) and whiskers (20 GPa), CNTs were expected to exhibit similar values of strength and stiffness [19]–[21]. CNTs possess high flexibility and high strength along with high stiffness. Young's modulus measured for individual arc-grown MWCNTs (26-76 nm diameter) using AFM were measured to be 1.28 ± 0.59 GPa [22]. Bending strength of MWCNTs were measured to be 14.2 ± 0.8 GPa. For the composites prepared using CNTs, load transfer from the matrix to CNTs is considered as the most important factor. Hence the adhesion between the

matrix material and CNTs needs to be strong without inducing greater defects in the CNTs. For MWCNT, high thermal conductivity of about 3000 W/mK at room temperature which is twice as high as that of diamond at 1000 W/mK and 10 times that of copper have also been demonstrated [19].

1.6.2 Engineering applications

Due to the physical properties discussed above, MWCNTs have been shown to exhibit enhanced performance in various engineering applications. The exceptional mechanical properties (Young's modulus, tensile strength etc.) of MWCNTs are very promising for being used in composite synthesis. Due to their nanosize, clearly defined morphology and structure, high electrical conductivity and chemical stability, they were demonstrated to be used in flat panel displays and screens. CNTs have been reported to have high, reversible hydrogen storage ability and hence can be used as a hydrogen storage medium. MWCNTs are not quite extensively used in commercial applications today. However several potential applications are currently being researched. Recently, MWCNTs have been shown to exhibit Li-intercalation ability with very high capacity and cycling capability for hundreds of cycles. The high cyclability of CNT is due to the amount of Li-ions that can be inserted between the concentric nanotubes. The high electrical conductivity in CNTs results in faster cycling of the electrodes and therefore CNTs are being extensively investigated as a filler material for anodes in Li-ion batteries. CNTs have also been proposed for use as field effect transistors, single electron transistors, diodes, gas sensors, water purification and biomedical applications [23].

1.7 Polymer Derived Ceramic Structure

Due to the remarkable physical and mechanical properties, carbon nanotubes are being considered to be one of the most promising new reinforcements for structural composites. Their

exceptional electrical and thermal properties also make them a good fit for multifunctional applications. Carbon nanotubes have been used as fillers in various ceramic matrices to overcome the intrinsic brittleness and lack of mechanical reliability. In addition to mechanical effects, the CNT reinforcing phase, may benefit other properties such as electrical conductivity, thermal expansion co-efficient, hardness and thermal shock resistance [24], [25]. The combination of these characteristics with intrinsic advantages of ceramic materials such as high temperature stability, high corrosion resistance, light weight and electrical insulation makes CNT-Ceramic composites highly attractive as functional and structural materials for a variety of high temperature or harsh environment applications. Since carbon nanotubes agglomerate and form bundles due to Van der Waals force as shown in Fig 1-10, they are extremely difficult to disperse and align in a polymer matrix.

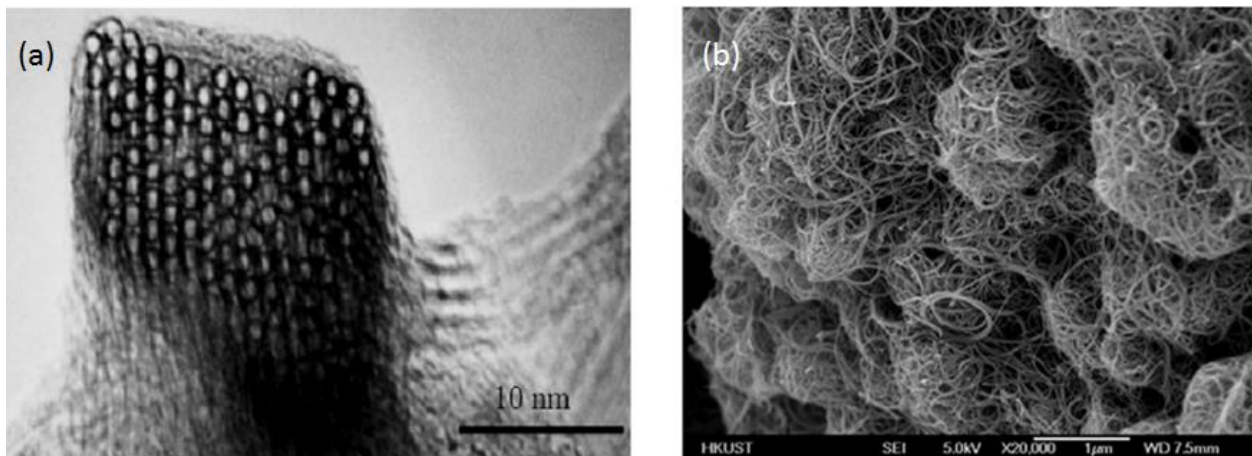


Figure 1-10: SEM images of (a) Single wall nanotube bundle (b) Entangled multiwall carbon nanotube agglomerates [26].

The mechanical dispersion methods such as ultra-sonication of CNTs in solvents (organic/aqueous) do not result in a stable suspension. The functionalization of CNT is an effective way to prevent nanotube aggregation, which helps to better disperse and stabilize the

CNTs within a polymer matrix. The functionalization of CNT is an effective way to prevent nanotube aggregation, which helps to better disperse and stabilize the CNTs within a polymer matrix. There are basically two approaches to functionalize CNTs; 1) covalent functionalization of functional groups onto the π -conjugated CNT surface. The drawback with this method is that, it changes the sp^2 carbon to sp^3 carbon at the functionalization sites thereby losing the desired properties of the CNTs. 2) Non-covalent functionalization of nanotubes on the other hand, does not compromise the physical properties of CNTs, but improves solubility and processability. This type of functionalization mainly involves surfactants, bio-macromolecules or wrapping with polymers. The polymer wrapping process as illustrated in Fig 1-11 is achieved through the van der Waals interactions and π - π stacking between CNTs and polymer chains containing aromatic rings. Another kind non-covalent functionalization is the endohedral method in which guest atoms or molecules such as C_{60} , Ag, Au, Pt are stored in the inner cavity of CNTs through the capillary effect.[26], [27]

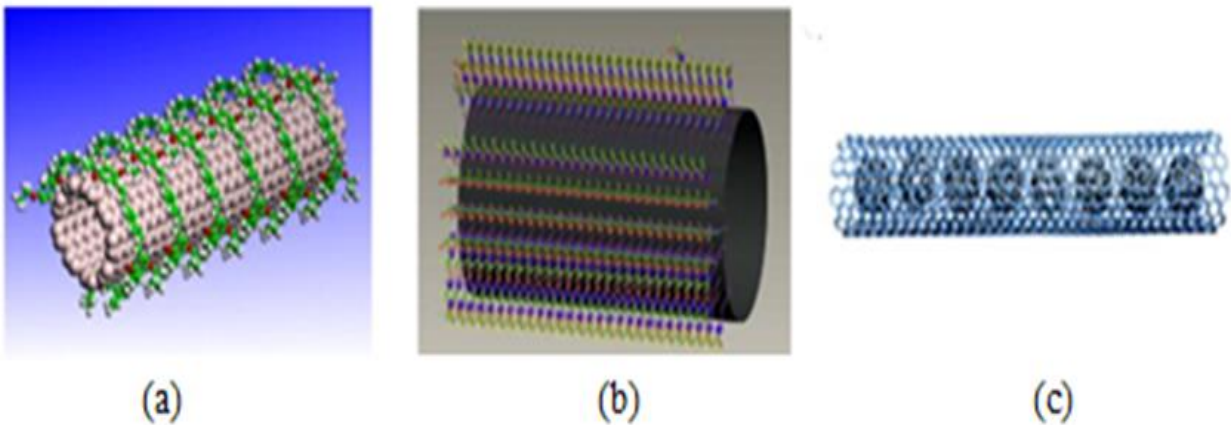


Figure 1-11: A schematic showing the various non-covalent functionalization methods (a): polymer wrapping (b) Surfactant adsorption (c) Endohedral method [26].

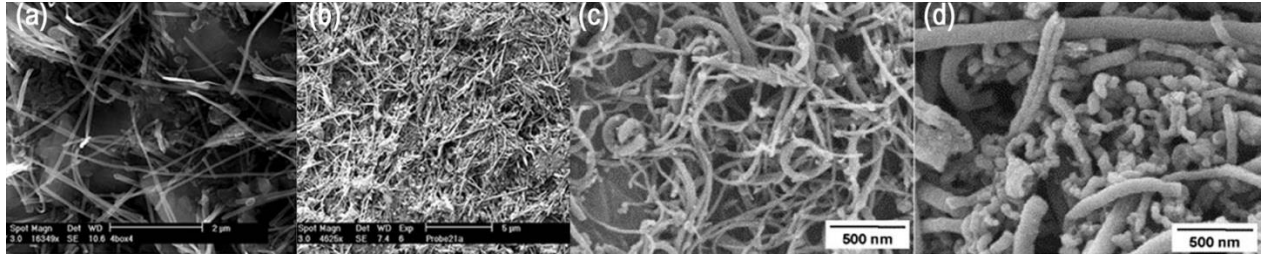


Figure 1-12: (a-b) SEM image of fracture surface of SiCN/CNT composite with 10 and 5 vol % CNT respectively [28], [29]. (c-d) SEM image of SiCN/MWCNT composite nanowires [30].

Composites using carbon nanotubes and ceramics such as SiC, Al₂O₃ etc. were studied by several groups before (Figure 1-9). These methods involved less interaction between the nanotubes and ceramics and hence possessed improved functional properties [28]–[31]. Duan et al proposed a novel approach to synthesize amorphous SiCNO nanowires by interfacing PDC and CNT in a liquid phase by the heat treatment of polymer functionalized nanotubes [30]. Later, a similar approach was followed to synthesize SiCN-CNT [14], [32], [33] and SiOC-CNT [34]–[36] composites. Subsequently various properties of these novel PDC-CNT composites were investigated and the findings were very promising as shown in Table 1-1. Several engineering applications, demand high performance and multifunctional properties from the material. In this report, composites using PDC starting from an aluminium doped polymeric precursor, and CNTs were synthesized and their high temperature performance were studied. Later the application of the synthesized composite material as a high temperature coating was also demonstrated.

Table 1-1: Various properties of PDC-CNT composites studied previously.

Property Studied	Investigators	Findings
Mechanical Property (elasticity)	Linan <i>et al.</i>	Addition of CNTs resulted in increased stiffness of the composite [14].
Electromechanical response	Shah <i>et al.</i>	SiCN/CNT specimens exhibited both higher sensitivity and linear response to the input load [33].
Fracture toughness	Katsuda <i>et al.</i>	Studied the reinforcement to the SiCN/CNT composite via fracture toughness behavior, which remained uniform with increasing crack length [32].

1.8 Application: Laser Thermal Detector Coatings

The rising needs for the use of high energy lasers in applications such as optical lithography, laser welding and cutting, laser surgery and military devices calls for an accurate calibration of the incident radiation for operation accuracy. Calorimetric methods which involve the conversion of incident laser energy to heat at the surface of a radiation absorbent material are most commonly used to calibrate these lasers. The next generations of high-power industrial and military lasers requires operation at power densities exceeding $10\text{kw}/\text{cm}^2$. This demands the development of better thermally stable materials which are good optical absorbents as well. Calorimeters can be broadly classified into isoperibol type (heated surface is thermally insulated) and conduction type (heated surface is cooled by a flowing water jacket) calorimeters. The conduction type calorimeters, results in a lower temperature drop across the absorbing material, thereby providing the ability for high irradiance measurements. The one shown in Fig 1-14 (a) is a conduction type liquid flow calorimeter in which the optical laser energy is converted into heat

on the surface of the radiation absorbing cone-shaped copper cavity which is coated with carbon nanotubes.

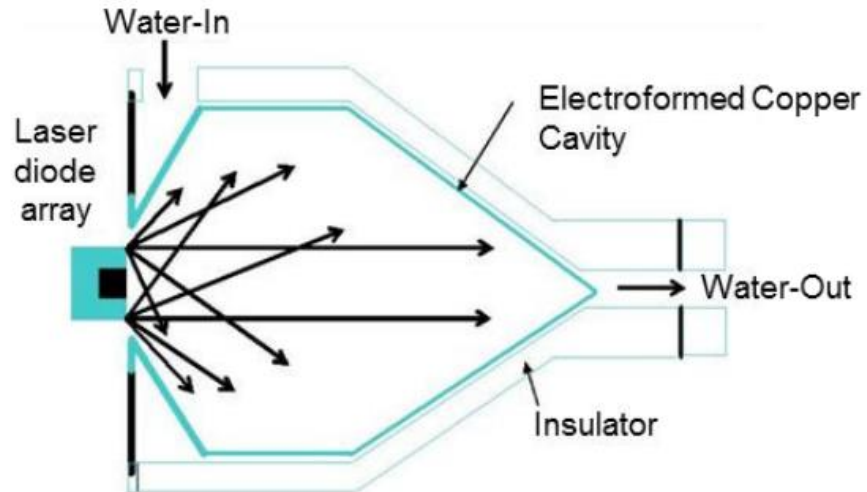


Figure 1-13: Cutaway diagram of the flowing-water thermal detector, illustrating the absorbing cavity and the water-flow channel on the outer surface of the cavity [37].

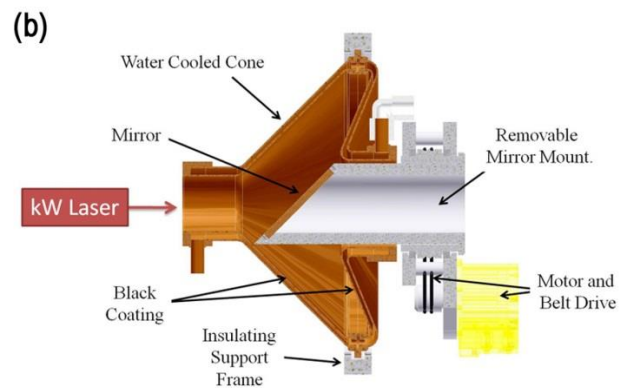


Figure 1-14: (a) A cone cavity coated with carbon nanotubes as the coating material [38]. (b) A schematic showing the conduction type liquid flowing type calorimeter with various parts labeled [39].

The cavity is surrounded by a flowing water jacket which absorbs the heat transferred by the black coating inside the cavity wall. Under steady state conditions the following parameters are typically known.

1. The mass flow rate of the water, \dot{m} in kg/s
2. The increase in temperature of the flowing water, $\Delta T = T_i - T_o$, where T_i is the inlet temperature and T_o is the outlet temperature
3. The specific heat capacity of water, $C_p = 4.198$ kJ/kg.K

Hence the power of the incident laser beam can be obtained from Equation 1-1 as follows

$$P_{laser} = \dot{m} \times C_p \times \Delta T \quad \text{Equation 1-1}$$

The reflected laser power at a given wavelength from the black coating can be measured in a separate set of experiments by using a power meter and low laser power. Thus the laser power can be precisely determined. In order to achieve maximum accuracy, an optimum coating material is desired to possess certain function properties such as shown in Table 1-2.

Table 1-2: Desired properties for the thermal absorbent coating materials for laser power meters.

Desired Property	Reason
High thermal conductivity	For effective transmission of absorbed heat to the substrate
Absolute zero reflectivity in the visible spectrum	For accurate response and to prevent coating damage due to laser attenuation
High visual damage threshold	For visual identification of the instance of damage

The commonly used coating materials for laser thermal detectors consists of carbon based paints, diffuse metal (gold black, silver black), oxidized metals (anodized aluminium) etc. because of their absorption of a broad range of wavelength (up to 40 μm) [1], [40]. These coating materials are not suitable for high power laser radiometry because of their poor laser damage threshold (or low oxidation resistance) [41], [42]. These materials also exhibit a non-uniform spectral response with reflectance ranging from 10%-20% [43], which is undesirable. Recently the use of carbon nanotubes as a coating material in the laser cone cavity showed an improved absorption efficiency and good thermal conductivity. Therefore a composite material made by coating carbon nanotubes (CNT) with PDC could improve its high temperature performance, thus enabling the calibration of lasers with higher powers. The PDC composite coating on the nanotubes will improve the thermal stability of the nanotubes thus improving the damage threshold of the coating material, compared to the bare carbon nanotube coatings shown in Fig 1-14. The Si(Al)CN-CNT composite coatings prepared in the report were sent to the National Institute of Standards and Technology (NIST) to evaluate its performance as a coating material in ultra-high power laser meters. The results of their study would help in future research in this direction.

1.9 References

- [1] N. Nelms and J. Dowson, “Goldblack coating for thermal infrared detectors,” *Sens. Actuators Phys.*, vol. 120, no. 2, pp. 403–407, May 2005.
- [2] C. L. Cromer, K. E. Hurst, X. Li, and J. H. Lehman, “Black optical coating for high-power laser measurements from carbon nanotubes and silicate,” *Opt. Lett.*, vol. 34, no. 2, p. 193, Jan. 2009.
- [3] Y. Wang, Y. Fan, L. Zhang, W. Zhang, and L. An, “Polymer-derived SiAlCN ceramics resist oxidation at 1400 °C,” *Scr. Mater.*, vol. 55, no. 4, pp. 295–297, Aug. 2006.
- [4] P. Colombo, *Polymer Derived Ceramics: From Nano-structure to Applications*. DEStech Publications, Inc, 2010.
- [5] P. Colombo, G. Mera, R. Riedel, and G. D. Sorarù, “Polymer-Derived Ceramics: 40 Years of Research and Innovation in Advanced Ceramics,” *J. Am. Ceram. Soc.*, vol. 93, no. 7, pp. 1805–1837, 2010.
- [6] W. Verbeek, “US Patent,” 3,853,867,1974.
- [7] M. Takamizawa, T. Kobayashi, A. Hayashida, and Y. Takeda, “US Patent,” 4604367 (1984).
- [8] A. E. Abel, T. A. Kruger, R. W. Mouk, and G. J. Knasiak, “Silazane and/or polysilazane compounds and methods of making,” 632948711-Dec-2001.
- [9] Y. D. Blum, A. L. Dodge, R. M. Laine, J. M. Mcleod, R. M. Platz, D. L. Roberts, D. J. Rowcliffe, and K. B. Schwartz, “Polysilazanes and related compositions, processes and uses,” WO1987005298 A111-Sep-1987.
- [10] D. Seyferth and G. H. Wiseman, “Preceramic organosilazane polymers,” 448266913-Nov-1984.

- [11] P. A. Ramakrishnan, Y.-T. Wang, D. Balzar, L. An, C. Haluschka, R. Riedel, and A. M. Hermann, "Silicoboron carbonitride ceramics: A class of high-temperature, dopable electronic materials," *Appl. Phys. Lett.*, vol. 78, no. 20, pp. 3076–3078, 2001.
- [12] R. Riedel, A. Kienzle, W. Dressler, L. Ruwisch, J. Bill, and F. Aldinger, "A silicoboron carbonitride ceramic stable to 2,000°C," *Nature*, vol. 382, no. 6594, pp. 796–798, Aug. 1996.
- [13] L. A. Liew, R. A. Saravanan, V. M. Bright, M. L. Dunn, J. W. Daily, and R. Raj, "Processing and characterization of silicon carbon-nitride ceramics: application of electrical properties towards MEMS thermal actuators," *Sens. Actuators -Phys.*, vol. 103, no. 1–2, pp. 171–181, Jan. 2003.
- [14] L. N. An, W. X. Xu, S. Rajagopalan, C. M. Wang, H. Wang, Y. Fan, L. G. Zhang, D. P. Jiang, J. Kapat, L. Chow, B. H. Guo, J. Liang, and R. Vaidyanathan, "Carbon-nanotube-reinforced polymer-derived ceramic composites," *Adv. Mater.*, vol. 16, no. 22, p. 2036–+, Nov. 2004.
- [15] L. An, Y. Wang, L. Bharadwaj, L. Zhang, Y. Fan, D. Jiang, Y.-H. Sohn, V. H. Desai, J. Kapat, and L. C. Chow, "Silicoaluminum carbonitride with anomalously high resistance to oxidation and hot corrosion," *Adv. Eng. Mater.*, vol. 6, no. 5, pp. 337–340+275, 2004.
- [16] S. Iijima, "Helical microtubules of graphitic carbon," *Nature*, vol. 354, no. 6348, pp. 56–58, Nov. 1991.
- [17] "Carbon nanotube," *Wikipedia, the free encyclopedia*. 16-Oct-2013.
- [18] A. Javey, R. Tu, D. B. Farmer, J. Guo, R. G. Gordon, and H. Dai, "High Performance n-Type Carbon Nanotube Field-Effect Transistors with Chemically Doped Contacts," *Nano Lett.*, vol. 5, no. 2, pp. 345–348, Feb. 2005.

- [19] R. W. Cahn, "Physics of graphite: B.T. Kelly (Applied Science Publishers, London, 1981) pp. 477. price: £48," *J. Nucl. Mater.*, vol. 114, no. 1, p. 116, Feb. 1983.
- [20] A. Kelly and N. H. Macmillan, *Strong solids*. Clarendon Press, 1986.
- [21] R. Bacon, "Growth, Structure, and Properties of Graphite Whiskers," *J. Appl. Phys.*, vol. 31, no. 2, pp. 283–290, 1960.
- [22] E. W. Wong, P. E. Sheehan, and C. M. Lieber, "Nanobeam Mechanics: Elasticity, Strength, and Toughness of Nanorods and Nanotubes," *Science*, vol. 277, no. 5334, pp. 1971–1975, Sep. 1997.
- [23] V. N. Popov, "Carbon nanotubes: properties and application," *Mater. Sci. Eng. R Rep.*, vol. 43, no. 3, pp. 61–102, Jan. 2004.
- [24] K. K. Chawla, *Composite Materials: Science and Engineering*. Springer.
- [25] F. L. Matthews and R. D. Rawlings, *Composite Materials: Engineering and Science*. Woodhead Publishing, 1999.
- [26] N. G. Sahoo, S. Rana, J. W. Cho, L. Li, and S. H. Chan, "Polymer nanocomposites based on functionalized carbon nanotubes," *Prog. Polym. Sci.*, vol. 35, no. 7, pp. 837–867, Jul. 2010.
- [27] P.-C. Ma, N. A. Siddiqui, G. Marom, and J.-K. Kim, "Dispersion and functionalization of carbon nanotubes for polymer-based nanocomposites: A review," *Compos. Part Appl. Sci. Manuf.*, vol. 41, no. 10, pp. 1345–1367, Oct. 2010.
- [28] R. Z. Ma, J. Wu, B. Q. Wei, J. Liang, and D. H. Wu, "Processing and properties of carbon nanotubes-nano-SiC ceramic," *J. Mater. Sci.*, vol. 33, no. 21, pp. 5243–5246, Nov. 1998.

- [29] G.-D. Zhan, J. D. Kuntz, J. Wan, and A. K. Mukherjee, "Single-wall carbon nanotubes as attractive toughening agents in alumina-based nanocomposites," *Nat. Mater.*, vol. 2, no. 1, pp. 38–42, Jan. 2003.
- [30] R.-G. Duan and A. K. Mukherjee, "Synthesis of SiCNO Nanowires Through Heat-Treatment of Polymer-Functionalized Single-Walled Carbon Nanotubes," *Adv. Mater.*, vol. 16, no. 13, pp. 1106–1109, 2004.
- [31] S. Berber, Y. K. Kwon, and D. Tomanek, "Unusually high thermal conductivity of carbon nanotubes," *Phys. Rev. Lett.*, vol. 84, no. 20, pp. 4613–4616, May 2000.
- [32] Y. Katsuda, P. Gerstel, N. Janakiraman, J. Bill, and F. Aldinger, "Reinforcement of precursor-derived Si-C-N ceramics with carbon nanotubes," *J. Eur. Ceram. Soc.*, vol. 26, no. 15, pp. 3399–3405, 2006.
- [33] S. R. Shah and R. Raj, "Nanodevices that explore the synergies between PDCs and carbon nanotubes," *J. Eur. Ceram. Soc.*, vol. 25, no. 2–3, pp. 243–249, 2005.
- [34] Y. Wang, Z. Iqbal, and S. Mitra, "Rapid, low temperature microwave synthesis of novel carbon nanotube–silicon carbide composite," *Carbon*, vol. 44, no. 13, pp. 2804–2808, Nov. 2006.
- [35] M. Pashchanka, J. Engstler, J. J. Schneider, V. Siozios, C. Fasel, R. Hauser, I. Kinski, R. Riedel, S. Lauterbach, H.-J. Kleebe, S. Flege, and W. Ensinger, "Polymer-Derived SiOC Nanotubes and Nanorods via a Template Approach," *Eur. J. Inorg. Chem.*, vol. 2009, no. 23, pp. 3496–3506, 2009.
- [36] M. Luo, Y. Li, S. Jin, S. Sang, and L. Zhao, "Oxidation resistance of multi-walled carbon nanotubes coated with polycarbosilane-derived SiC_xO_y ceramic," *Ceram. Int.*, vol. 37, no. 8, pp. 3055–3062, Dec. 2011.

- [37] K. Ramadurai, “Carbon nanostructures for thermal applications: Synthesis and characterization,” Ph.D., University of Colorado at Boulder, United States -- Colorado, 2007.
- [38] N. US Department of Commerce, “New Nanotube Coating Enables Novel Laser Power Meter.” [Online]. Available: http://www.nist.gov/pml/div686/laser_050509.cfm. [Accessed: 23-Oct-2013].
- [39] N. US Department of Commerce, “Laser Radiometry: Powering Up.” [Online]. Available: http://www.nist.gov/pml/div686/laser_power_meter.cfm. [Accessed: 23-Oct-2013].
- [40] D. J. Advena, V. T. Bly, and J. T. Cox, “Deposition and characterization of far-infrared absorbing gold black films,” *Appl. Opt.*, vol. 32, no. 7, pp. 1136–1144, Mar. 1993.
- [41] H.-J. Kleebe, “Microstructure and Stability of Polymer-Derived Ceramics; the Si–C–N System,” *Phys. Status Solidi A*, vol. 166, no. 1, pp. 297–313, 1998.
- [42] K. Ramadurai, C. L. Cromer, A. C. Dillon, R. L. Mahajan, and J. H. Lehman, “Raman and electron microscopy analysis of carbon nanotubes exposed to high power laser irradiance,” *J. Appl. Phys.*, vol. 105, no. 9, p. 093106, May 2009.
- [43] J. H. Lehman, K. E. Hurst, L. K. Roberson, K. Nield, and J. D. Hamlin, “Inverted Spectra of Single-Wall Carbon Nanotube Films,” *J. Phys. Chem. C*, vol. 112, no. 31, pp. 11776–11778, Aug. 2008.
- [44] J. F. Moulder and J. Chastain, *Handbook of X-Ray Photoelectron Spectroscopy: A Reference Book of Standard Spectra for Identification and Interpretation of XPS Data*. Perkin-Elmer Corporation, Physical Electronics Division, 1992.

Chapter 2 - Study of Si(Al)CN Functionalized Carbon Nanotube Composite as a High Temperature Thermal Absorber Coating Material

2.1 Introduction

Polymer derived ceramics and carbon are of interest to synthesize advanced composites due to their multifunctional properties. Carbon nanotubes (CNT) are known to possess excellent mechanical strength and thermal conductivity, but they tend to get oxidized in air at around 400°C. Polymer derived ceramics (PDC) on the other hand are amorphous ceramics which show high temperature stability (up to ~1400°C). Here we demonstrate the synthesis of a PDC-CNT composite structure consisting of a CNT core with a ceramic shell outside. Such a hybrid structure would prevent the oxidation of carbon nanotubes at lower temperatures and hence will retain their properties at high temperatures. This was achieved through a novel process involving an aluminum modified liquid precursor through a reaction of aluminum isopropoxide and poly(ureamethylvinyl)silazane under normal conditions; followed by the conversion of polymer to ceramic on carbon nanotube surfaces through controlled heating.

2.2 Preparation of the Pre-Ceramic Polymer

The preceramic polymer was prepared by the addition of Polyureamethylvinyl silazane (Commercially known as Ceraset) to Aluminium isopropoxide in the ratio of 10:1. 5g of preceramic polymer was required for 0.5 g of CNT to prepare the final CNT-ceramic composite. In order to obtain a uniform combination of the polymer components Aluminum isopropoxide

was added to 20ml toluene and stirred using a magnetic stirrer for about 20 min. The Ceraset was later added to this solution and stirred again so that it formed a uniform mixture. Now the preceramic polymer is ready to be added to the carbon nanotubes.

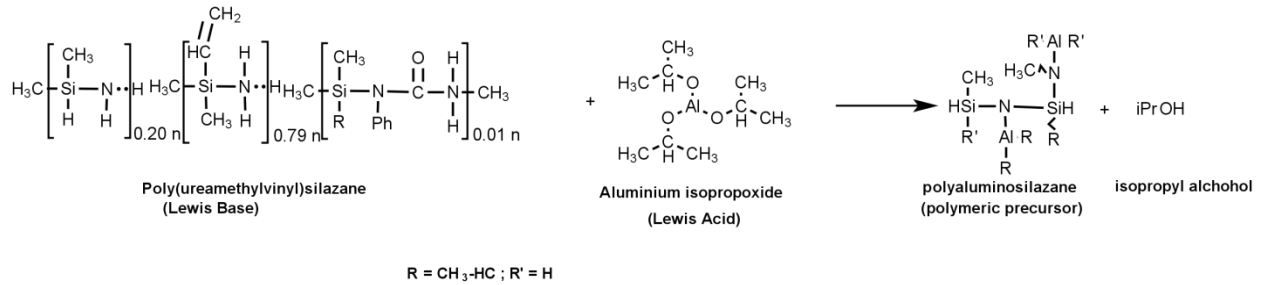


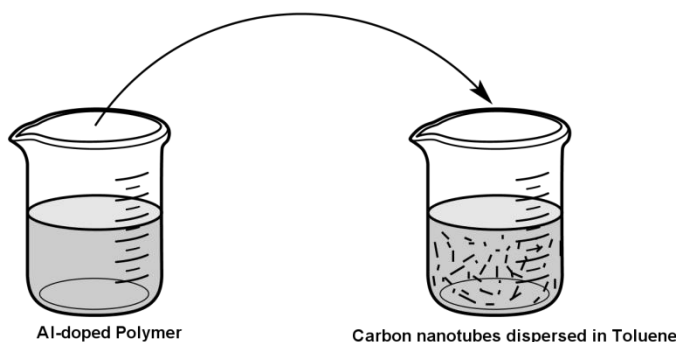
Figure 2-1: Proposed reaction mechanism for molecular level interfacing of Aluminium with poly(ureamethylvinyl)silazane liquid polymer.

The commercially obtained Carbon nanotubes tend to form bundles, which results in poor dispersion and are not desired when functionalized with a polymer. Therefore the nanotubes were mixed with NADDBS (an anionic surfactant) which would non-covalently functionalize the nanotubes on the walls thus resulting in a uniform dispersion which is required for our purpose [2]. The carbon nanotubes were mixed with NADDBS in 1:1 ratio and added to 200ml distilled water. This mixture was put into in a bath sonicator for 1hr and then poured into a vacuum filtration setup. The dried and dispersed nanotubes were collected in the filter within 48 hours which was collected by carefully scraping it off the filter paper. The collected CNTs were then added to 200 ml toluene and then sonicated for 30 min. The Al-modified polymer was then added to this mixture and then stirred again for 1hr. After the stirring is over the mixture was dried by keeping it inside an oven at 84°C as shown in Fig 2-2. The dried residue was collected after 24 hours. The residue would be a CNT-Polymer mixture which can be pyrolyzed later to obtain the final CNT-ceramic mixture.

1. Aluminium isopropoxide is added dropwise to the ceraset



2. The preceramic polymer is added to the CNT-Toluene mix



3. The CNT-Polymer mix is now transferred into an oven at 84°C

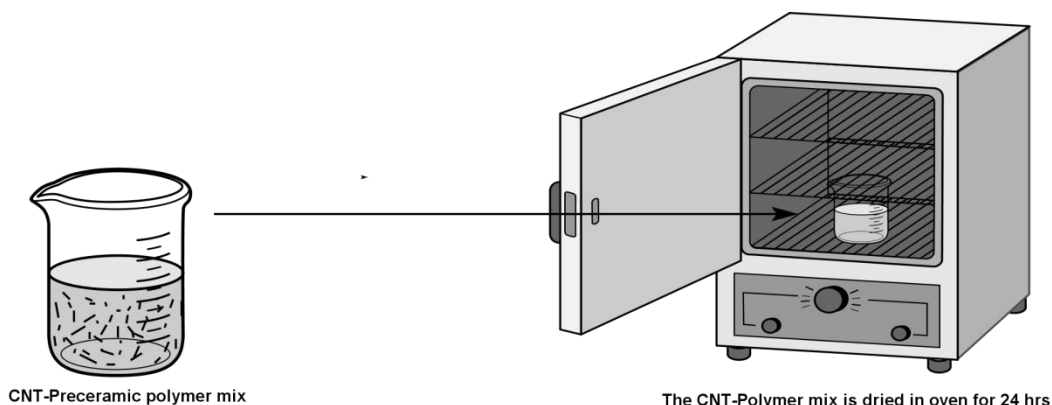


Figure 2-2: Schematic showing the preparation of the CNT-Preceramic polymer mixture

2.3 Conventional Pyrolysis

The conventional method employed for the pyrolysis of preceramic polymers involves the heating of the sample in a tube furnace under nitrogen flow at ~ 25 mL/min. As shown in Fig 2-3, the heating rates are set in the furnace such that the powder is cross-linked at 400°C for 90 min and pyrolyzed at 800°C for 4h. The heating rate for cross-linking was set to $2^{\circ}\text{C}/\text{min}$ and the heating rate for pyrolysis was set to $5^{\circ}\text{C}/\text{min}$. After the pyrolysis is complete, the powder is cooled to room temperature in typically 5hrs or more.

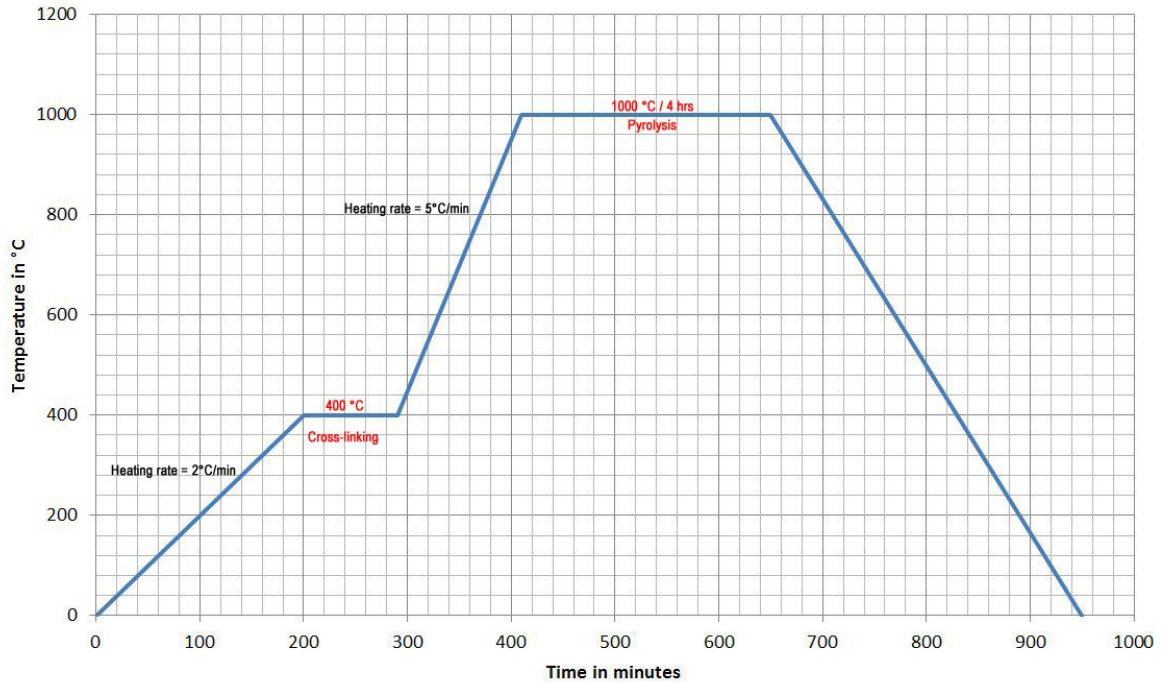


Figure 2-3: Graph showing the heating rates during the cross-linking and pyrolysis of the preceramic polymer.

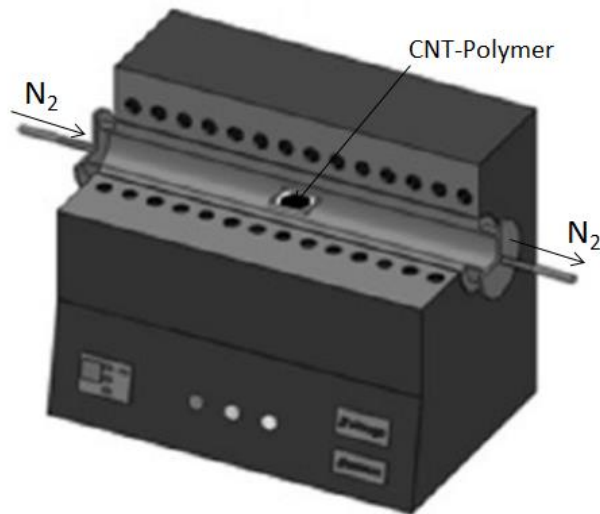


Figure 2-4: Schematic showing the conventional pyrolysis of the CNT-Polymer mix in the tube furnace with flowing nitrogen.

The various gases such as CH₄ (methane) and C₂H₆ (Ethane) are evolved during this pyrolysis due to the release of oligomers from the polymer structure. These gaseous by products are removed by the continuous flow of nitrogen gas through the tube as shown in Fig 2-4 and exhausted through a fume hood. This method of pyrolysis is time and energy consuming. Alternative methods of heating such as microwave heating are hence desirable as a source of heat for the faster and economic ceramization of the preceramic polymer.

2.4 Microwave Pyrolysis

Microwave pyrolysis can only be used as the heat source for the ceramization of preceramic polymers, when a “microwave absorbing” filler phase is available in the polymer matrix. This is due the fact that polymers alone would not absorb microwaves and hence cannot be heated by microwave absorption [3]. This makes a carbon nanotube-preceramic polymer hybrid matrix a perfect fit to be employed in a microwave assisted pyrolysis. Carbon nanotubes have shown to exhibit high microwave absorption accompanied with rapid temperature increase up to 2000°C [1]. This knowledge can be used to employ microwave irradiation as a medium to heat the nanotubes in the CNT-Polymer mix thus converting the polymer coated CNT to a ceramic CNT. A conventional microwave oven (Model: Emerson MW9325SL) was modified so that a test tube could be inserted into the microwave chamber. The CNT-Polymer composite was placed at the bottom of the test tube and the test tube was purged with nitrogen gas for approximately 5 min before the microwave. The nitrogen would create an inert atmosphere so that the oxidation of CNT is prevented during the reaction. One gram of as prepared CNT-Polymer composite powder was placed in a test tube and inserted into the microwave chamber as shown in Fig 2-5. The samples were exposed to microwaves at full power (900W @ 2.5GHz). The reaction was

accompanied by the formation of sparks inside the material and the heating up of the bottom surface of the test tube which clearly indicated the sudden generation of heat within the material.

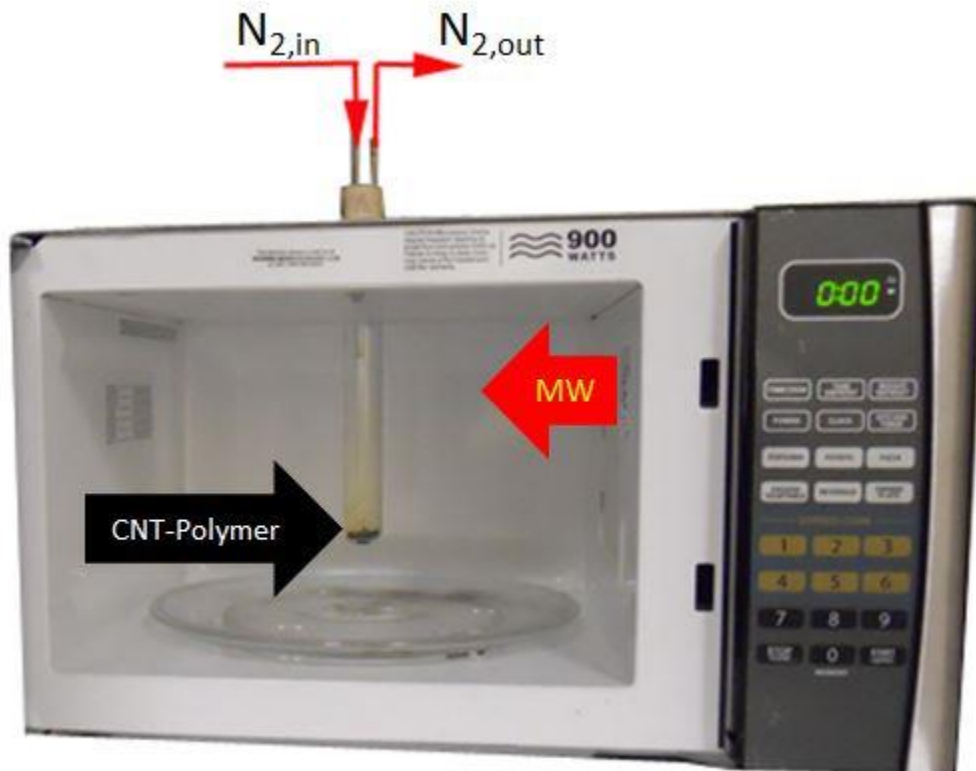


Figure 2-5: A photograph showing the experimental setup for the microwave pyrolysis of the preceramic polymer. The black material at the bottom of the test tube is the CNT-Polymer mix. The yellow fumes seen indicate the release of ammonia.

2.5 Characterization

Electron Microscopy: SEM was performed using Carl Zeiss EVO Low-Vacuum SEM and FEI Nova NanoSEM 430. TEM was performed using Philips CM 100 (100 KeV) and FEI Tecnai F20 XT (200 KeV) for high-resolution imaging.

TGA: Thermogravimetric analysis was performed using Shimadzu 50 TGA (limited to 1000 °C). Sample weighing, approximately 3 mg, was heated in a platinum pan at a rate of 10 °C/min in air flowing at 20 mL/min.

Raman Spectroscopy: Thermo Scientific DXR Raman microscope with an air-cooled green Nd:YAG laser ($\lambda = 532$ nm) of 5 mW power was used as excitation source for all the specimens. Spectra were collected on the instrument operating with 3.1 μm confocal hole size, 50 μm wide entrance slit, 900 grating lines/mm and 10X MPlan objective Olympus lens. Data processing was performed using Thermo Scientific's Omnic software for microRaman. The samples were mounted on a manually controlled x-y stage.

2.5.1 Electron microscopy

Transmission electron microscopy (TEM) is a high resolution microscopic technique that uses a beam of electrons transmitted through a given specimen. The image formed is a result of the interaction of the electrons transmitted through the specimen which is magnified and focused onto a fluorescent screen or detected by a sensor such as a CCD camera. Transmission electron microscopy of the Si(Al)CN/MWCNT composite specimen obtained after pyrolysis as shown in Fig 2-6 confirmed the formation of composite nanowires consisting of Si(Al)CN shell on MWCNT core. The transmission electron microscope diffraction pattern was featureless thus confirming the amorphous nature of the prepared composite ceramic

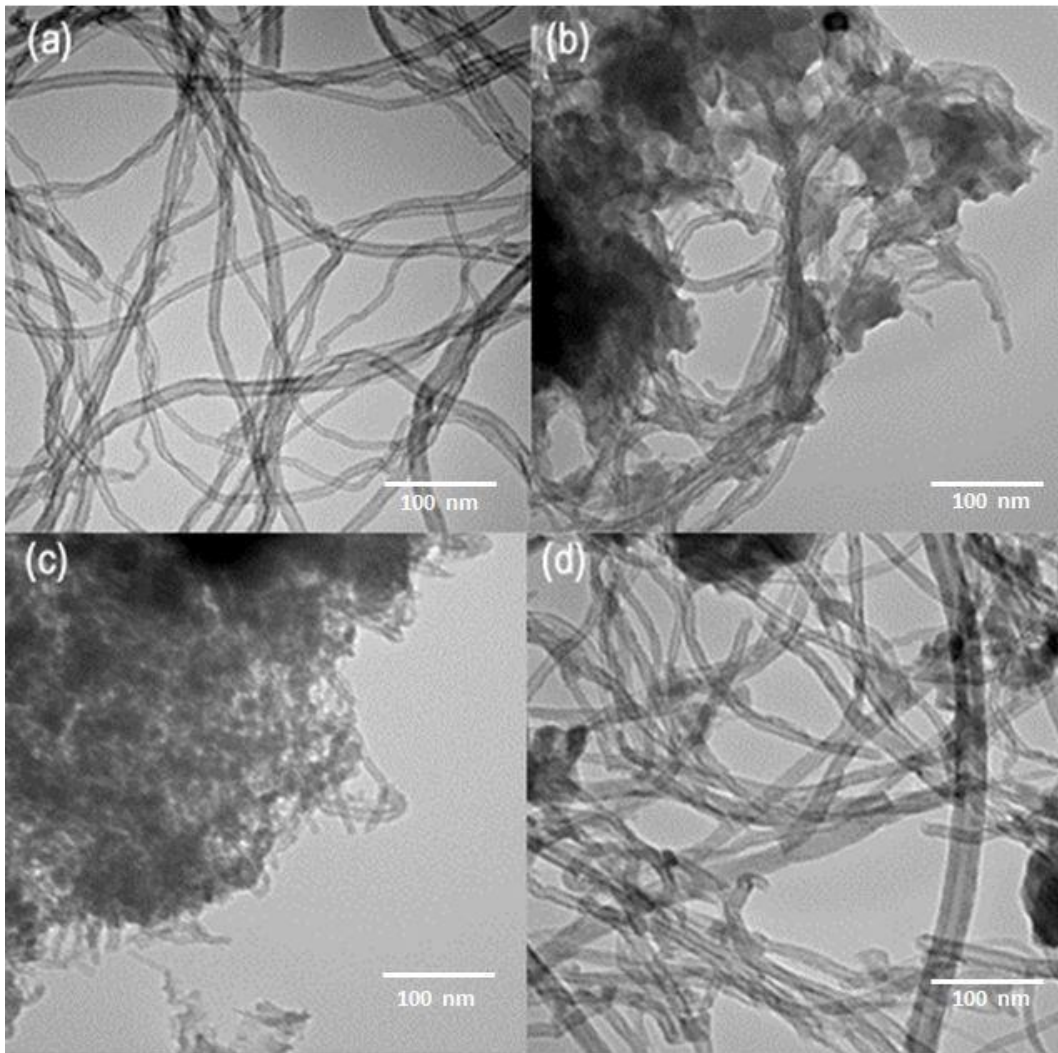


Figure 2-6: TEM images (a) bare nanotubes (b) Polymer coated nanotubes (c) Nanotube-ceramic prepared by the conventional method (d) CNT-ceramic prepared by microwave pyrolysis.

2.5.2 Thermogravimetric analysis

Thermogravimetric analysis (TGA) is a method of thermal analysis in which changes in physical and chemical properties of materials are measured as a function of increasing temperature (with constant heating rate), or as a function of time (with constant temperature and/or constant mass loss). The TGA instrument continuously weighs a sample as it is heated to

temperatures of up to 1000° C. As the temperature increases, various components of the sample are decomposed and the weight percentage of each resulting mass change can be measured. Results are plotted with temperature (°C) on the X-axis and weight loss (%) on the Y-axis. TGA can be used to evaluate the thermal stability of a material. In a desired temperature range, if a species is thermally stable, there will be no observed mass change. Negligible mass loss corresponds to little or no slope in the TGA trace. Thermogravimetric analysis was performed for Si(Al)CN-CNT composite synthesized by conventional heating, Si(Al)CN-CNT synthesized by microwave heating, as well as for pristine MWCNTs in order to compare their high temperature behavior.

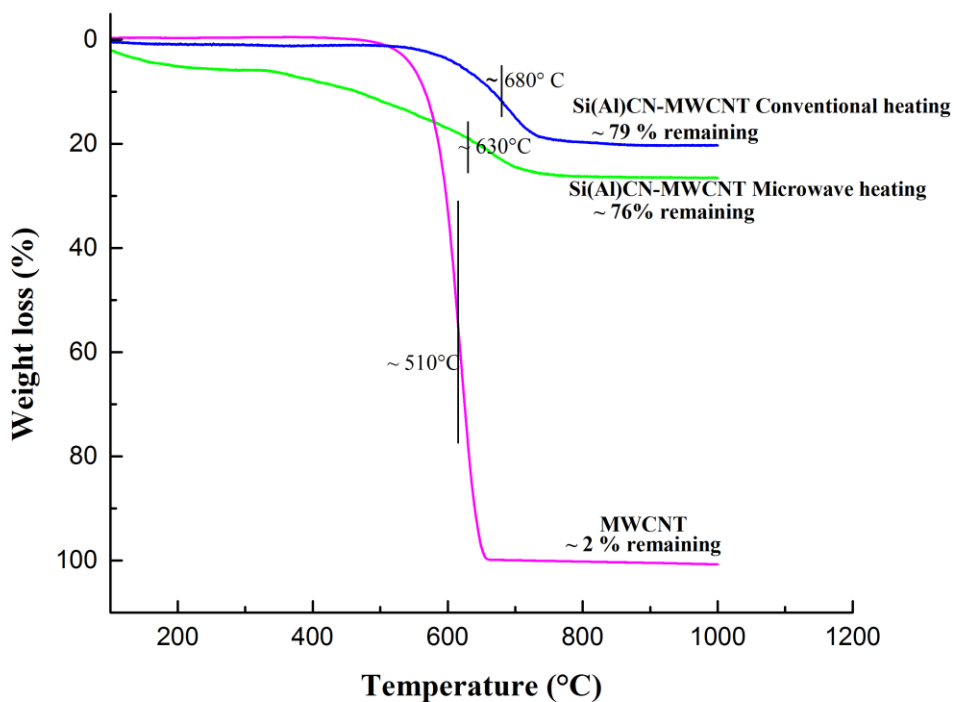


Figure 2-7: (a) TGA plots showing the weight loss (%) and oxidation temperature ($^{\circ}\text{C}$) for MWCNT, Si(Al)CN-MWCNT prepared by conventional heating, Si(Al)CN-MWCNT prepared by microwave heating and MWCNTs performed in flowing air.

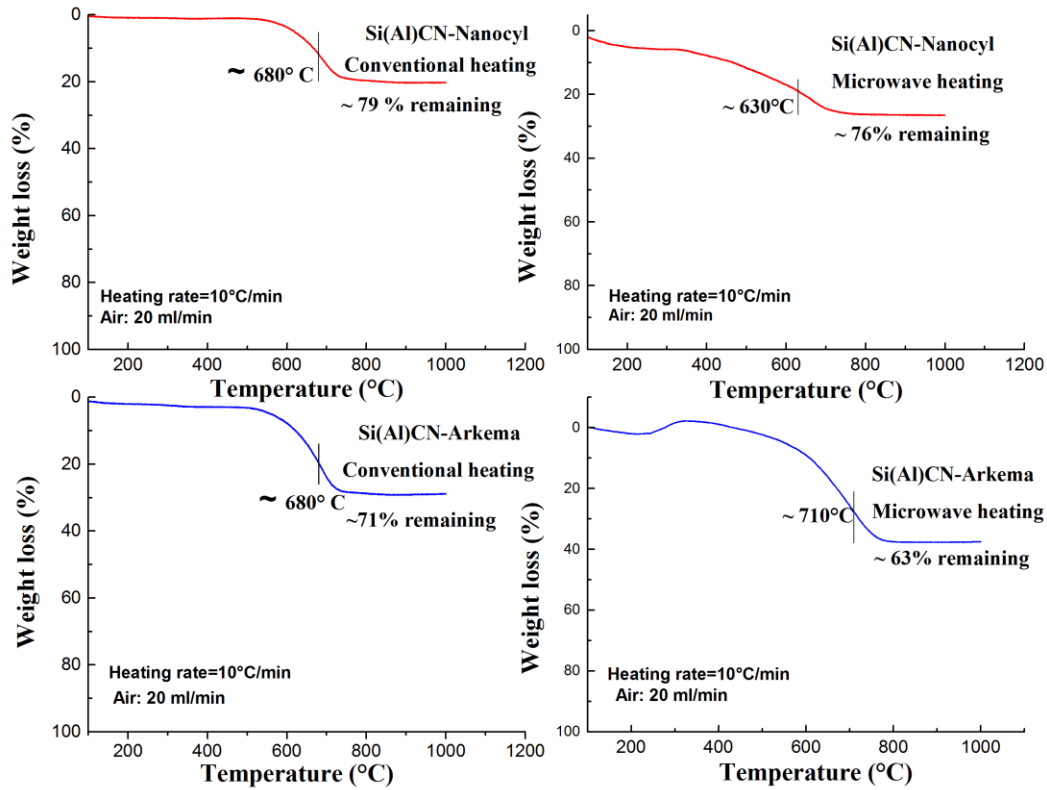


Figure 2-8: TGA plots showing the weight loss (%) and oxidation temperature ($^{\circ}\text{C}$) for the two varieties of Si(Al)CN-MWCNT composites prepared by using two commercially available MWCNT (Manufacturer1: Nanocyl and Manufacturer2: Arkema), synthesized through both conventional and microwave heating.

As shown in Fig 2-7, the Si(Al)CN-MWCNT specimens had a linear relationship between residual mass and the oxidation temperature, which was observed around $750 \pm 10^{\circ}\text{C}$. After the

weight loss at about 750°C, the composite nanowire specimen showed stability in their weight which suggests that the composite retained their unique structure at high temperatures. The TGA residual weight was 79% for Si(Al)CN specimen synthesized by conventional heating and 76% for Si(Al)CN specimen synthesized by microwave heating. The TGA data for bare nanotubes on the other hand indicate 98% weight loss at ~510°C. Thus the composite structure prepared by the coating the bare nanotubes with Si(Al)CN ceramic has shown improved oxidation resistance by around 150°C. The narrow weight loss range of pristine nanotubes suggested that they were formed of homogenous material whereas an extended weight loss range for the composite nanowire sample implies a larger range of oxidation temperature with lesser weight loss of a comparatively non-homogenous amorphous ceramic. The (25%–30%) weight loss for Si(Al)CN-MWCNT composite nanowires could be attributed to the combustion of small diameter, defective or non-uniformly coated nanotubes. Thus TGA proves the improved thermal stability of the Si(Al)CN/MWCNT composite as compared to bare nanotubes.

2.5.3 Raman spectroscopy

Raman spectroscopy is one of the spectroscopic techniques which are available for the analysis of materials and chemicals. It relies on Raman scattering of light by a material, where the light is scattered inelastically as opposed to the more prominent elastic Rayleigh scattering. This inelastic scattering causes shifts in wavelength, which can then be used to deduce information about the material. Properties of the material can be determined by analysis of the spectrum, and/or it may be compared with a library of known spectra to identify a substance. The Raman spectroscopy of the prepared Si(Al)CN-MWCNT composite powder displayed characteristic peaks around D band (1350 cm^{-1}) and G band (1600 cm^{-1}) as shown in Fig 2-9 which corresponds to the D and G bands typical of CNT. This confirms the presence of CNT in the

final ceramic. The presence of CNT in the final composite material is very crucial in order to utilize its desirable functional properties for various applications.

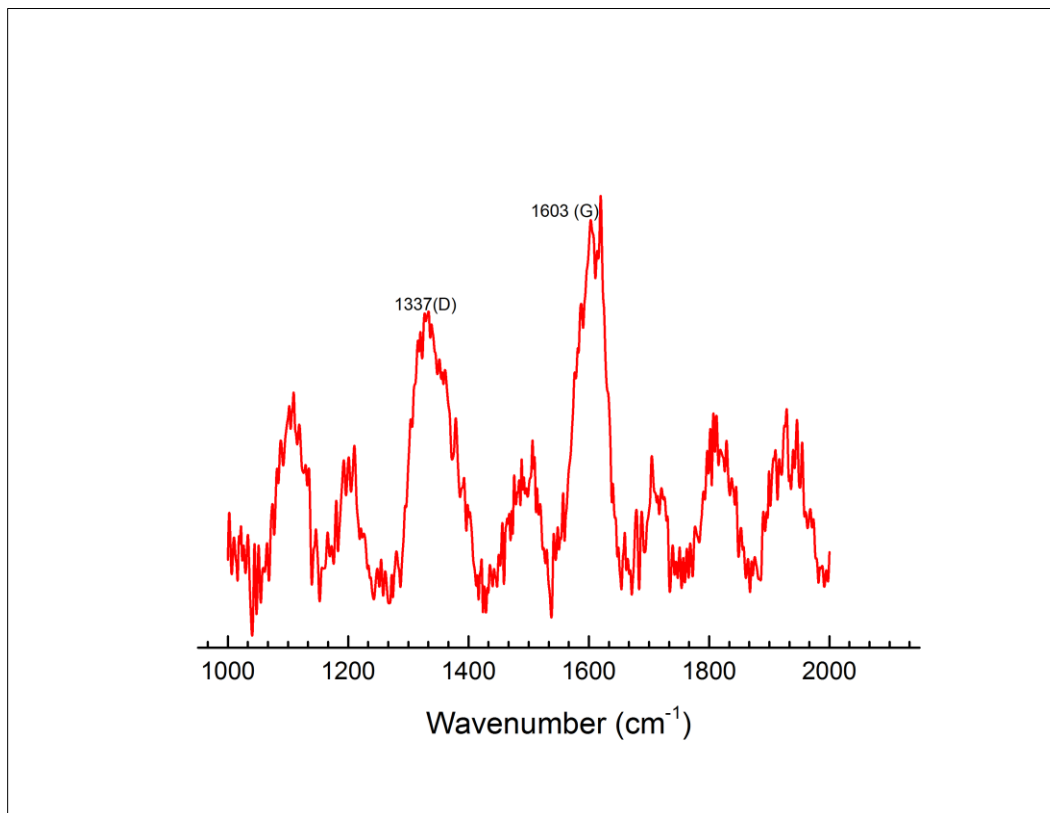


Figure 2-9: Raman spectra of the as prepared Si(Al)CN/CNT composite. The Raman plot of Si(Al)CN-MWCNT ceramic composite powder indicates the presence of D (~1350 cm⁻¹) and G (~1600 cm⁻¹) bands (peaks) that are characteristic of carbon nanotubes (CNT).

2.5.4 X-ray photoelectron spectroscopy

XPS provides deterministic information about the nature of bond formation and the percentage of elements constituting a compound. The X-ray spectra is obtained by exposing a material maintained in ultra-high vacuum, to a beam of x-rays, while simultaneously measuring the kinetic energy and the number of electrons that escape from the top 0 to 12 nm of the material being analyzed. The XPS spectrum is a plot of the number of electrons (Plotted along the Y-axis)

versus the binding energy (in eV) of the electrons detected (Plotted along the X-axis). The peaks obtained are compared against standard spectral values established to interpret the data.

The XPS spectrum of the Si(Al)CN-MWCNT composite material revealed distinct peaks from which the elemental composition of the final material was confirmed. The survey scans of the specimen showed the existence of Si, Al, and C elemental peaks arising from the valence energy levels for the respective atoms. The peak at about 74.4 eV for the high resolution Al_{2p} spectrum as shown in Fig 2-10 confirmed the presence of Aluminium in the final composite material [4]. This proves the successful introduction of Aluminium into the final ceramic material. The binding energy of the C_{1s} photoelectrons as shown in Fig 2-11 at ~284.5 eV suggest a sp² carbon peak [4][44][44]. This suggests the presence of sp² bonded free carbon in the final composite material. The emergence of a distinctive peak at about ~101.8 eV in the Si_{2p} spectrum as shown in Fig 2-12 indicated the formation of Si-N bond (Si₃N₄) [4].

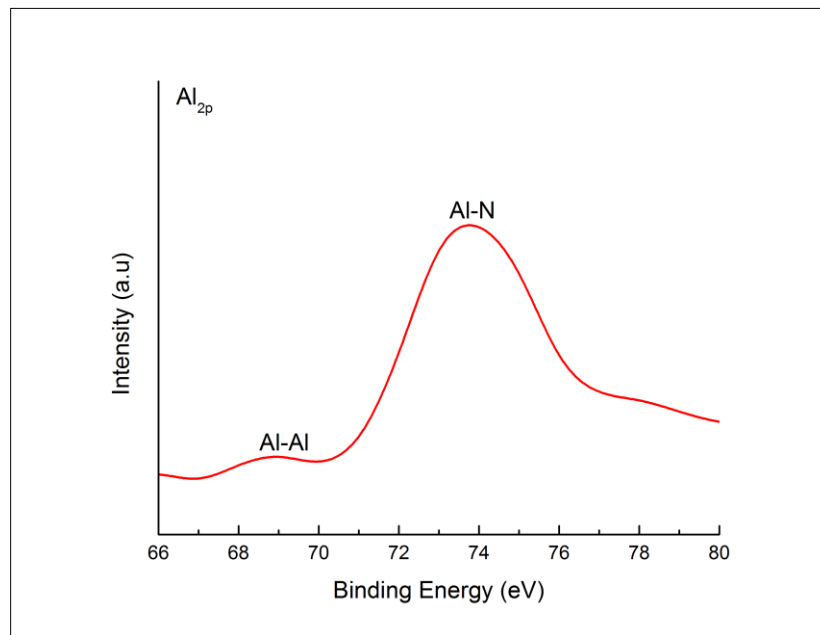


Figure 2-10: High resolution Al_{2p} XPS spectrum. The peak at 74.4 eV is indicative of the presence of Al-N bonds in the final ceramic.

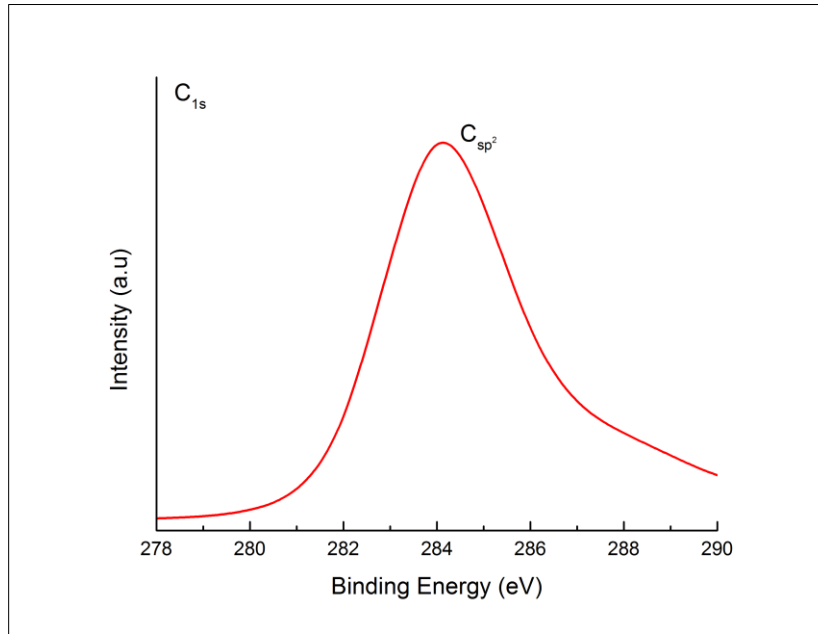


Figure 2-11: High resolution C_{1s} XPS spectrum indicating the presence of sp^2 bonded graphitic carbon at around 284.5 eV.

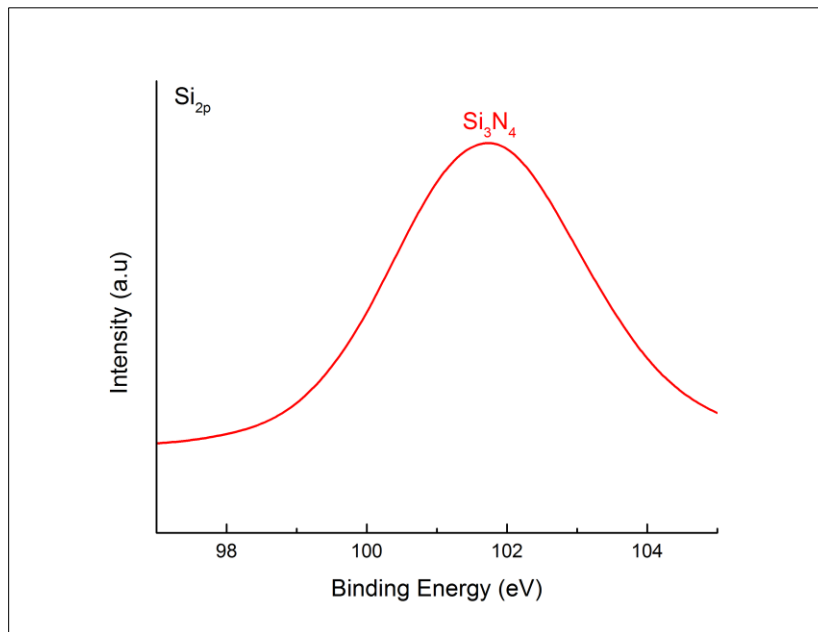


Figure 2-12: High resolution Si_{2p} XPS spectrum of the composite material shows a characteristic peak at 101.8 eV indicating the presence of Si₃N₄.

2.6 Preparation of Coatings

The Si(Al)CN/MWCNT composite material was gently crushed using mortar-pestle to obtain a fine powder (approximately 1 to 2 μm in size, as determined by the SEM). It was then dispersed in toluene (ACS reagent) and sonicated for 1 h to obtain uniform dispersions as shown in Fig 2-13. These dispersions were later carefully sprayed on copper substrates by use of an airbrush (Model: Paasche-H#1) at 15 psi air. The spraying was done with longitudinal passes (with a single pass lasting for approximately 5 s followed by 10 s of break) while the substrate surface temperature was raised to 80 °C. Frequent stops between the passes allowed the solvent to evaporate and thereby form a uniform compact coating. Spray coating was carried out until the appropriate dark black coating thickness was visually realized, with an approximate thickness of 10 μm. The coated copper disks were then maintained at 100°C on a hot plate for 12 h to ensure removal of volatile components.

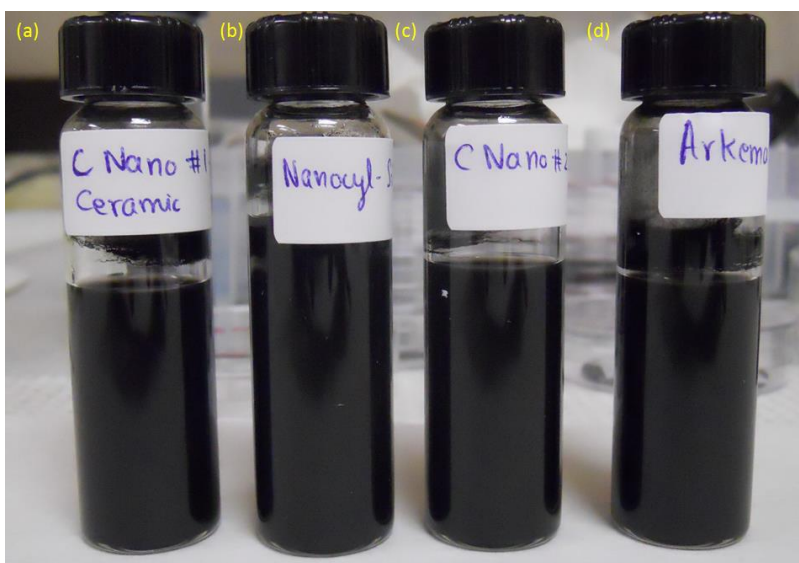


Figure 2-13: Photograph showing the dispersions of Si(Al)CN-MWCNT composite powder in toluene prepared by using four different commercially available makes of MWCNTs (a) Si(Al)CN-C Nano #1 b) Si(Al)CN-Nanocyl c) Si(Al)CN-C Nano #2 d) Si(Al)CN-Arkema

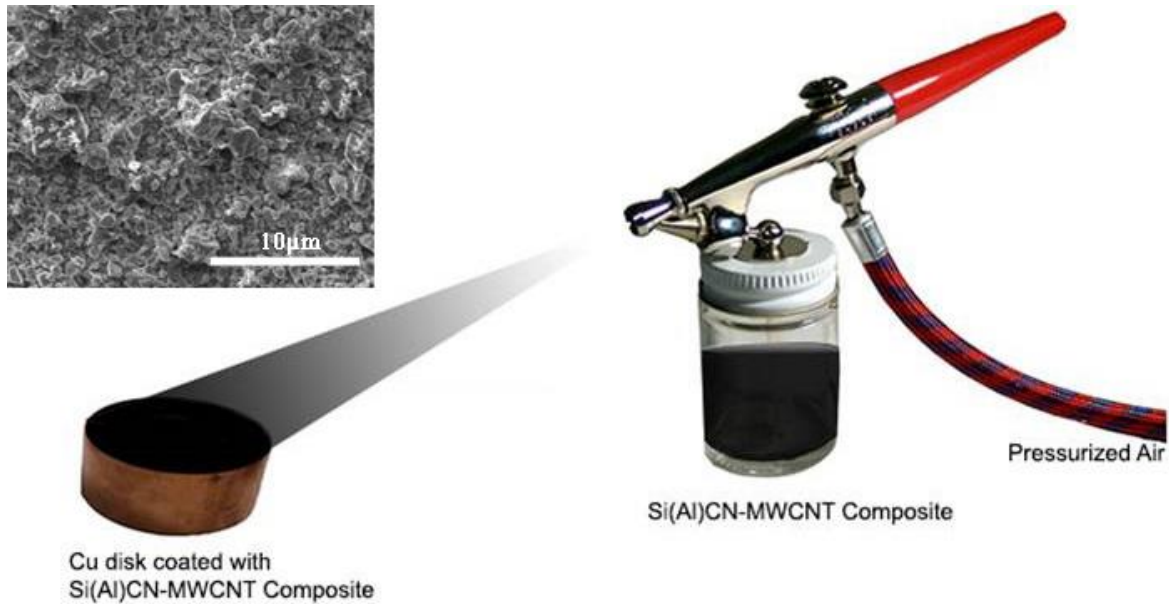


Figure 2-14: A schematic showing the spray coating of the copper disks with the as prepared CNT-Ceramic composite. (Inset is the SEM image of the coating showing the uniform distribution of the particles on the surface of the coating).

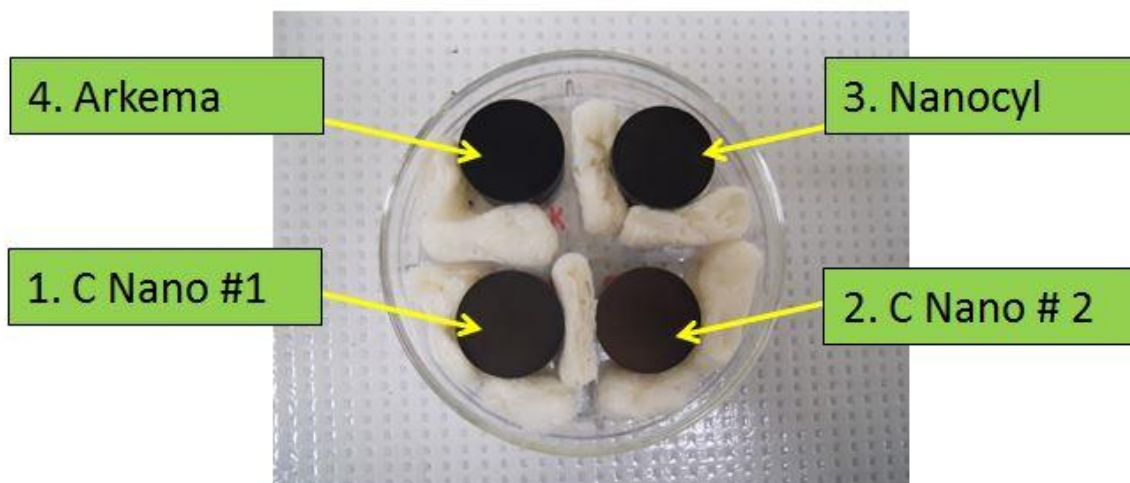


Figure 2-15: A photograph showing the four Si(Al)CN-MWCNT coatings prepared by using

four different commercially available makes of MWCNTs. This would help in comparing the effect of different varieties of CNT on the thermal performance of the coating.

The copper disk with large mass would be assumed as an infinite heat sink, a close representation of the actual calorimetric cone used for laser calibration as shown in Fig 1-14. Therefore the disk specimens could be used to test the performance of the prepared coating, as a thermal absorber material in laser power meters. Details on the laser experimental setup are available in reference [5]. The composite coated copper disk specimens were sent to National Institute of Standards and Technology, for evaluating their performance as a thermal absorber coating in laser power meters. Various parameters such as the laser damage threshold would be studied which will be helpful for future research in this direction.

2.7 References

- [1] T. Imholt, C. A. Dyke, B. Hasslacher, J. M. Pérez, D. W. Price, J. Roberts, J. B. Scott, A. Wadhawan, Z. Ye, and J. M. Tour, “Nanotubes in Microwave Fields: Light Emission, Intense Heat, Outgassing, and Reconstruction,” *Chemistry of Materials*, vol. 15, no. 21, pp. 3969–3970, Sep. 2003.
- [2] P.-C. Ma, N. A. Siddiqui, G. Marom, and J.-K. Kim, “Dispersion and functionalization of carbon nanotubes for polymer-based nanocomposites: A review,” *Composites Part A: Applied Science and Manufacturing*, vol. 41, no. 10, pp. 1345–1367, Oct. 2010.
- [3] P. Colombo, *Polymer Derived Ceramics: From Nano-structure to Applications*. DEStech Publications, Inc, 2010.
- [4] J. F. Moulder and J. Chastain, *Handbook of X-Ray Photoelectron Spectroscopy: A Reference Book of Standard Spectra for Identification and Interpretation of XPS Data*. Perkin-Elmer Corporation, Physical Electronics Division, 1992.
- [5] K. Ramadurai, C. L. Cromer, A. C. Dillon, R. L. Mahajan, and J. H. Lehman, “Raman and electron microscopy analysis of carbon nanotubes exposed to high power laser irradiance,” *Journal of Applied Physics*, vol. 105, no. 9, p. 093106, May 2009.

Chapter 3 - Conclusion and Future Work

We have reported the successful introduction of aluminium into a polysilazane polymer precursor following a single-step process. This was achieved through a reaction of aluminium isopropoxide with polyureasilazane under atmospheric conditions. The aluminium modified preceramic polymer which is liquid at room temperature was then interfaced with carbon nanotube surfaces to form Si(Al)CN/MWCNT shell/core nanowires. TEM images confirmed the formation of nanowires and the amorphous nature of the ceramic shell. Detailed spectroscopic studies revealed the presence of Si-N, Al-N bonds and the presence of sp^2 bonded free carbon which is desirable for its functional properties such as high temperature stability and thermal conductivity. Thermogravimetric studies showed that the composite material was stable at high temperatures upto 1000°C showing a high residual mass to weight loss ratio.

We have also demonstrated the preparation of spray coatings composed of Si(Al)CN-MWCNT composite that will be used in ultra-high temperature applications such as laser calorimetry. The spray coated disks were sent to NIST for further evaluation of the performance of the coatings as a thermal absorbent coating material for application in laser power meters.

PDC-CNT composites have also been reported as a suitable material to be used as a high electrochemical capacity electrode in rechargeable batteries, due to its lithium intercalation abilities. The performance study of the as prepared Si(Al)CN/MWCNT composite material as an anode material and an analysis of the performance of such batteries could be an interesting study for the future.